Modelling and exergy analysis of the natural gas to hydrocarbon liquids (GTL) process

by

Johann Adriaan Venter

A report submitted in partial fulfillment
of the requirements for the degree

Master of Engineering

in the

Faculty of Engineering, the Built Environment and Information Technology

University of Pretoria

Pretoria

31 October 2002

Synopsis

The interest in using Fischer–Tropsch synthesis for converting natural gas to liquids has increased during the last couple of years. Most of the technologies are well established individually, but integrating these technologies have not been applied and optimised widely. Firstly process integration was performed on a Gas-to-Liquids (GTL) process consisting of an autothermal reformer (ATR) and low temperature slurry bed reactor (SBR) with external recycling. Secondly the interactions of the integrated GTL process were investigated with specific focus on factors influencing the carbon efficiency. It was evident that a trade–off exists between carbon efficiency, methane slip and energy utilization. Exergy analysis was used as optimization tool and resulted in an optimum ATR temperature of 975°C. The results showed that at the optimum temperature the methane slip (2.7%) is still within an acceptable range. When comparing the optimum ATR temperature to a temperature of 1100°C, the improvement in carbon efficiency is 7% and the total exergy loss is 26% lower. At this optimum ATR temperature the energy is utilized in such a manner that the maximum exergy is stored in the final product (i.e. liquid hydrocarbons) and not in utilities (i.e. electricity) produced by the process.

Keywords

Gas-to-Liquids, exergy, reforming, Fischer–Tropsch, process integration, carbon efficiency, process optimization

Contents

List of Figures

Nomenclature

$\dot{m}$	Mass flow rate of fluid stream, kg/s
$\dot{Q}_r$	Heat transfer rate, W
$\dot{W}_x$	Shaft power, W
$\dot{W}_{max}$	Maximum work, W
$\varepsilon^{\Delta P}$	Pressure dependent component of exergy streams with regards to physical exergy, W
A	Area for heat transfer, m^2
C_0	Bulk velocity of fluid stream relative to surface of earth, m/s
g_E	Gravitational acceleration, $kg/m \cdot s^2$
H_0	Enthalpy at T_0, kJ/mol
H_1	Enthalpy at given state, kJ/mol
I	Irreversibility, W
k_1	Reaction constant for first FT reaction mechanism (Lox & Froment, 1993)
k_5	Reaction constant for fifth FT reaction mechanism (Lox & Froment, 1993)
k_6	Reaction constant for sixth FT reaction mechanism (Lox & Froment, 1993)
n	Carbon chain length
p	Alpha value
P_0	Reference pressure, bar

Q	Heat, J
R	Gas contant, 8.314 $J/mol \cdot K$
S_0	Entropy at T_0, kJ/mol
S_1	Entropy at given state, $kJ/mol \cdot K$
T_0	Ambient temperature; standard temperature, K;$^\circ C$
T_r	Reactor/reaction temperature. K;$^\circ C$
T_{ref}	Temperature of ATR, K;$^\circ C$
U	Overall heat transfer coefficient. $W/m^2 \cdot K$; internal energy. J
x_i	Mole fraction of component i
y_n	Flory mole fraction distribution
Z_0	Altitude of stream above sea level, m
C_p	Heat capacity, $kJ/mol \cdot K$

Subscripts

0	Chemical
0	Environmental state (reference state)
E	Related to energy
i	Related to component i
k	Related to kinetic energy
m	Mean
max	Maximum
n	Carbon chain length
p	At constant pressure
p	Related to potential energy

ph	Physical
r	Related to rate
r	Related to reaction
ref	Reformer

Greek

α	Schulz-Flory alpha distribution
ΔT_m	Mean temperature - driving force for heat transfer, K
Δ	Change: (out-in) or (end-beginning)
$\Delta_r G^0$	Standard Gibbs energy of reaction, kJ/mol
$\Delta_r H^0$	Standard heat of reaction, kJ/mol
$\dot{\varepsilon}^{W_x}$	Exergy related to work, W
$\dot{\varepsilon}_{in}, \dot{\varepsilon}_{out}$	In and out going exergy material streams, W
$\dot{\varepsilon}$	Exergy of a stream of matter, W
$\dot{\varepsilon}^Q$	Thermal exergy, W
$\dot{\varepsilon}_0$	Chemical exergy, W
$\dot{\varepsilon}_k$	Kinetic exergy, W
$\dot{\varepsilon}_p$	Potential exergy, W
$\dot{\varepsilon}_{ph}$	Physical exergy, W
Π	Entropy production, $kJ/K \cdot s$
τ	Carnot factor
$\varepsilon^{\Delta T}$	Temperature dependent component of exergy streams with regards to physical exergy, W
$\varepsilon_{0,}$	Standard chemical exergy of component i, W

Superscripts

P	Dependent on pressure
Q	Related to heat
T	Dependent on temperature
W_x	Related to work

Abbreviations

ATR	Autothermal reformer
FT	Fischer–Tropsch
GTL	Gas–to–Liquids
HTFT	High temperature Fischer–Tropsch
LTFT	Low temperature Fischer–Tropsch
POX	Partial oxidation
SBR	Slurry bed reactor
SMR	Steam methane reforming
SSBR	Sasol Slurry Bed Reactor
syngas	Synthetic gas
TFBR	Tubular fixed bed reactor

Chapter 1

Introduction

1.1 Background

During the last couple of years , there has been a renewed interest in the use of Fischer-Tropsch technology for the conversion of natural gas to hydrocarbon liquids (GTL process). Some of the factors that contributed to this are (Vosloo, 2001):

1. An increase in the known reserves of natural gas.
2. The need to monetise remote or stranded natural gas.
3. Environmental pressure to minimise the flaring of associated gas.
4. Improvements in the cost-effectiveness of Fischer-Tropsch technology resulting from the development of more active catalysts and improved reactor designs.

The process to convert natural gas to hydrocarbon liquids can be divided into three process steps:

1. Syngas generation
2. Syngas conversion
3. Hydroprocessing

Although all three of the technologies for converting natural gas to hydrocarbon liquids are well established, individually optimised and commercially proven, the combined use is not widely applied (Vosloo, 2001). The optimal layout of the plant is determined by both economic and environmental aspects. Thus a balance have to be found between

minimising expensive unit processes (economic aspects) and negating environmental impacts. The Gas–to–Liquids (GTL) process would only be viable if capital cost could be reduced through integration (Hill, 1998). The integration of the three technologies for converting natural gas to liquids poses an interesting challenge to the designer. In order to make the GTL technology more competitive, the challenge goes beyond the optimization that deals only with the known aspects of these technologies. It also includes those aspects that are not commercialised yet and that may still be in the very early stages of development.

In this work an integrated GTL process design will thus be developed with specific focus on:

- optimization of product yield (i.e. maximum carbon efficiency) and
- minimum energy requirements.

A combination of process synthesis and exergy analysis will be used to reach these specific goals. The process synthesis will give the initial direction and identify the governing variables in the process. An exergy analysis will provide a sufficient approximation to the minimum energy requirements. In contrast to a mere energy study the exergy analysis also takes the thermodynamic quality of heat compared with other resources into consideration (Futterer *et al.*, 1996). In order to illustrate the applicability of the exergy concept and a way of presenting results of exergy analyses, computer-aided exergy analyses will be carried out for several process routes to find the optimum integrated GTL process. This work will only focus on the interaction between the syngas generation and syngas conversion process steps and will be referred to as the GTL process. The hydroprocessing units were not modelled and will thus not be included in this study.

Chapter 2

Literature survey

2.1 GTL processing steps

The GTL process has three main processing steps (see figure 2.1), all of which has been proven commercially (Lutz, 2001).

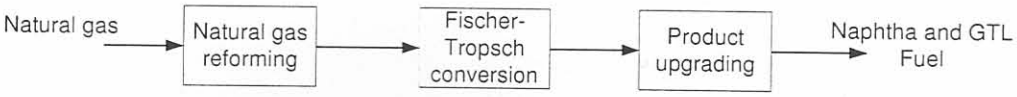

Figure 2.1: The basic GTL process

2.1.1 Natural gas reforming

This step converts natural gas (largely methane) into synthesis gas, also known as syngas (a mixture of hydrogen and carbon monoxide). The production of syngas is obtained by reforming natural gas with either steam or carbon dioxide, by partial oxidation or by a combination of the three. Due to the presence of water, the water gas shift reaction plays an important role.

The principal reactions of steam reforming are:

$$CH_4 + H_2O \rightleftharpoons CO + 3H_2, \qquad \Delta_r H^0 = 206.3 \frac{kJ}{mol} \tag{2.1}$$

$$CH_4 + CO_2 \rightleftharpoons 2CO + 2H_2, \qquad \Delta_r H^0 = 246.9 \frac{kJ}{mol} \tag{2.2}$$

$$CO + H_2O \rightleftharpoons CO_2 + H_2, \qquad \Delta_r H^0 = -40.6 \frac{kJ}{mol} \tag{2.3}$$

The principal partial oxidation reaction is:

$$CH_4 + \frac{1}{2}O_2 \rightarrow CO + 2H_2, \qquad \Delta_r H^0 = -35.6\frac{kJ}{mol} \tag{2.4}$$

The Fischer-Tropsch conversion step requires a stoichiometric H_2:CO ratio of about 2. The above mentioned reforming reactions give syngas with H_2:CO ratios ranging from less than 1 to more than 3. A combination of these reactions in the presence of a catalyst is normally practiced to obtain a suitable H_2:CO ratio. This may be done in a tubular catalytic steam reformer with a furnace to provide external heat, in an autothermal reformer where partial oxidation is combined with adiabatic catalytic steam reforming, or in a partial oxidation reformer followed by a shift reactor. When reforming is followed by Fischer-Tropsch (FT) conversion, it is possible to recycle FT tail gas to the feed of the reforming process in order to manipulate the H_2:CO ratio of the reformer outlet.

2.1.2 Fischer-Tropsch conversion

The second step, Fischer-Tropsch conversion, upgrades the syngas into waxy hydrocarbons by using the low temperature Fischer-Tropsch (LTFT) reactor. Originally LTFT was practiced in tubular fixed bed reactors. Currently Sasol in South Africa is using slurry phase reactors to overcome problems and limitations associated with tubular fixed bed reactors (Jager, 1998).

The simplified FT reaction can be represented as:

$$CO + 2H_2 \rightarrow -CH_2 - + H_2O, \qquad \Delta_r H^0 = -167.4\frac{kJ}{molCO} \tag{2.5}$$

Preheated syngas is fed to the bottom of the slurry reactor where it diffuses into the slurry. The syngas is converted into more wax by the FT reaction.

The lighter, more volatile fractions leave the reactor in a gas stream from the top of the reactor. The gas stream is cooled to recover the lighter cuts and water. The hydrocarbon streams (i.e. the wax and lighter cuts) are sent to the product upgrading unit, while the water stream is treated in the water recovery unit (Lutz, 2001).

2.1.3 Product upgrading

In the third step, the waxy syncrude is upgraded to middle distillate fuels: mainly GTL Fuel and some naphtha (Lutz, 2001).

The products from the slurry phase reactor are predominantly paraffinic, but the lighter products contain some olefins and oxygenates that need to be removed for product stabilization. Hydrogen is added to hydrotreat the olefins and oxygenates, thus converting them to paraffins. Hydrogen is also added to the mild hydrocracker, which breaks the long chain waxes into naphtha and GTL Fuel. The products are separated out in a fractionation section (Lutz, 2001).

In this study, the total product upgrading will not be considered. Only the first stage will be considered. The first stage of upgrading consists of cooling the gas stream to recover the lighter cuts and water. The lighter cuts is then recycled to the reformer or the FT reactor.

2.2 Background on Fischer-Tropsch synthesis

2.2.1 The low temperature Fischer-Tropsch (FT) reactor

Conversion of natural gas to Naphtha and GTL Fuel can be achieved by means of the FT process. The FT process can be operated at low temperatures (LTFT) to produce a syncrude with a large fraction of heavy, waxy hydrocarbons or it can be operated at higher temperatures (HTFT) to produce a light syncrude and olefins. With HTFT the primary products can be refined to environmentally friendly gasoline and diesel, solvents and olefins. With LTFT, the heavy hydrocarbons can be refined to speciality waxes. The heavy hydrocarbons can also be hydrocracked and/or isomerised to produce high quality diesel. It can also serve as base stock for lube oils and a naphta that is ideal feedstock for cracking to light olefins (Jager, 1998).

The composition of the hydrocarbon product fraction (-CH_2-) (see equation 2.5) can be described by the Schulz-Flory distribution. These products are then also known by trivial names in the industry, which can be seen in table 2.1.

2.2.2 The influence of CO_2 and H_2O on the Fischer–Tropsch reactor performance

Cobalt catalysts are more resistant towards reoxidation than iron based catalysts, but a certain degree of oxidation does still take place. The rate of oxidation of supported cobalt catalysts is a function of the operating temperature, partial pressure of water and crystallite size of the catalyst. Thus water will have a deactivation effect on the cobalt

Table 2.1: Trivial names of the main products of the FT synthesis

Chain Length	Trivial Name
C_{1-2}	Fuel Gas
C_{3-4}	LPG
C_{5-12}	Benzine
C_{5-10}	Naphtha
C_{11-13}	Kerosene
C_{13-17}	Diesel
C_{10-20}	Middle distillates
C_{19-23}	Soft waxes
C_{24-35}	Medium waxes
C_{35+}	Hard waxes

catalyst after long periods of operation (Espinoza *et al.*, 1999).

There is general consensus in the literature that carbon dioxide and water does not have an inhibiting effect on the rate of FT synthesis for catalysts that are not active for the water gas shift (WGS) reaction, such as the cobalt catalyst (Espinoza *et al.*, 1999). This is due to the fact that the FT rate for cobalt catalysts are more related to the ratio of the partial pressures of H_2:CO, while for iron catalysts it is more related to the absolute partial pressures of the reactants (Espinoza *et al.*, 1999).

In this study only the effect of the cobalt catalyst will be analysed.

2.2.3 The H_2:CO molar ratio and the Schulz-Flory alpha value in the Fischer-Tropsch reactor

The alpha value is the probability of carbon chain growth in the Fischer-Tropsch reactor. If the value is low and approaches zero, chain growth is not probable and the main product will be mainly methane. On the other hand, alpha approaches 1 and is high when longer carbon chains are formed.

For this study, the following equation was used to determine alpha (Lox & Froment, 1993):

$$\alpha = \frac{k_1 P_{CO}}{k_1 P_{CO} + k_5 P_{H_2} + k_6} \tag{2.6}$$

It can be seen from equation 2.6 that the alpha distribution will decrease with an increase in H_2:CO syngas ratio. The opposite is also true; the alpha distribution will increase with a decrease in H_2:CO syngas ratio.

The goal of the Fischer-Tropsch reactor in the GTL process is to make a product slate

with a typical alpha value of 0.95. This indicates that the product slate mainly consists of waxes (long carbon chains). These waxes can then be converted into many valuable products.

2.3 Existing technologies

2.3.1 Syngas generation

Fischer-Tropsch (FT) chemistry is often regarded as the key technological component of schemes for converting synthesis gas (or 'syngas') to transportation fuels and other liquid products. However, syngas production itself accounts for more than half the capital investment and a disproportionate share of the operating costs for a gas-to-liquids (GTL) complex. A recent study by SFA Pacific (see table 2.2) examines the full range of commercial and developmental synthesis gas production technologies and provides an independent assessment of syngas production options and costs for GTL applications (Karp *et al.*, 1998).

The manner in which syngas is produced can be influenced by, and in turn can profoundly impact, many facets of the overall GTL process design, such as (Wilhelm *et al.*, 2001):

- Plant size and location;
- The need for an oxygen plant or oxygen enrichment facilities;
- The physical size of downstream gas-handling equipment;
- Syngas composition and its associated effects on FT chemistry and yields;
- Heat integration and gas recycle options;
- Gas compression requirements;
- The scope and configuration of power generation alternatives.

This section examines the status of commercial and developmental syngas production technologies in the context of GTL production based on FT synthesis.

Syngas generation technologies

In principle, synthesis gas may be generated from any hydrocarbon feedstock. This is reflected in industrial practice, which includes large-scale syngas production from a wide variety of materials that includes natural gas, naphtha, residual oil, petroleum coke and coal. However, in the context of GTL applications, low–value natural gas is the predominant (if not the only) feedstock of interest (Wilhelm *et al.*, 2001).

In large part, this is a reflection of the high investment costs of GTL processes, which, in the absence of special circumstances, require a low or, even better, negative value feedstock to achieve attractive overall economics. Low quality residual oil or coke can have a low or even negative value. However, conversion of such feedstocks (via gasification) entails greater capital investment, in part due to the costs associated with materials handling, soot removal and syngas cooling and purification. The focus for GTL has thus been on associated gas, so-called stranded or remotely located gas reserves, and larger gas reserves that are not currently being economically exploited. In the near-term, associated gas may offer the greatest potential, particularly where such gas is subject to flaring constraints and associated reinjection costs (Wilhelm *et al.*, 2001).

The principal technologies for producing syngas from natural gas feed are summarized and compared in table 2.2. The predominant commercial technology for syngas generation has been, and continues to be, steam methane reforming (SMR), in which methane and steam are catalytically and endothermically converted to hydrogen and carbon monoxide. An alternative approach is partial oxidation, the exothermic, non-catalytic reaction of methane and oxygen to produce a syngas mixture. SMR and partial oxidation inherently produce syngas mixtures having appreciably different compositions. In particular, SMR produces a syngas having a much higher H_2:CO ratio. This, of course, represents a distinct advantage for SMR in hydrogen-production applications and, in large measure, accounts for its overall dominance among syngas production technologies to date (Wilhelm *et al.*, 2001).

As shown in table 2.3 and table 2.4, the product syngas composition from either process can, within limits, be manipulated by altering various process conditions and/or by means of additional process steps (Wilhelm *et al.*, 2001). Nonetheless, even with such manipulation; neither SMR nor partial oxidation is ideally suited to GTL applications. This is due to the fact that FT synthesis calls for an H_2:CO ratio of about 2, a value higher than that achievable with partial oxidation and lower than that obtainable with SMR.

A solution to this dilemma is to use both technologies. For example, partial oxida-

tion and SMR may be used in parallel to produce syngas streams that have differing compositions but, when mixed, form a total FT feedstock of the desired composition. An alternative to this approach is autothermal reforming (ATR), which combines partial oxidation with catalytic steam reforming in one reactor. The process is 'autothermal' in that the endothermic reforming reactions proceed with the assistance of the internal combustion or oxidation of a portion of the feed hydrocarbons-in contrast to the external combustion of fuel characteristic of conventional tubular reforming.

ATR properly refers to a stand-alone, single-step process for feedstock conversion to syngas. However, the same basic idea can be applied to reactors fed by partially reformed gases from a primary reformer. Such reactors form a subcategory of ATR that is commonly called secondary reforming. Due to feed composition differences-in particular, the lower concentration of combustibles in secondary reformer feeds-ATR reactors and secondary reformers have different thermal and soot-forming characteristics that require different burner and reactor designs. Nonetheless, the distinction between ATR and secondary reforming is not consistently drawn by technology users and vendors, with the result that secondary reformers often are referred to as ATRs (Wilhelm *et al.*, 2001).

Air-blown vs. oxygen-blown autothermal reforming

The importance of syngas production to overall GTL costs is vividly illustrated in Table 2.5, which shows the cost distribution for a facility that is based on the use of oxygen-blown ATR. As shown, GTL costs are dominated by capital charges, which comprise about two-thirds of the total costs. Syngas production, in turn, accounts for about half of the capital investment, in part due to the significant capital cost of the oxygen plant (Wilhelm *et al.*, 2001; Jager, 1998).

Not surprisingly, the oxygen plant investment has been an attractive target of GTL cost-cutting strategies. This target has spawned both long–term strategies (e.g., the previously mentioned ceramic membrane reactor) and short–term strategies (e.g., air-blown ATR). It remains to be seen how successful ceramic membrane reactor development will be. However, SFA Pacific sees no apparent advantage that would favour air-blown over oxygen-blown systems (Wilhelm *et al.*, 2001). Indeed, air-blown reforming technology is unlikely to be economically competitive with oxygen-blown systems and appears much less flexible. Factors which more than negate the savings associated with elimination of the oxygen plant include: lower thermal efficiency, high air compression power requirements, the inability (because of its composition) to recycle FT tail gas, and the larger downstream equipment sizes and pressure drop associated with handling the much larger

Table 2.2: Comparison of syngas generation technologies (natural gas feed)(Karp *et al.*, 1998)

Technology	Advantages	Disadvantages
SMR	Most extensive industrial experience	H_2:CO ratio often higher than required when CO also is to be produced
	Oxygen not required	Highest air emissions
	Lowest process temperature requirement	
	Best H_2:CO ratio for hydrogen production applications	
Heat exchange reforming	Compact overall size and 'footprint'	Limited commercial experience
	Application flexibility offers additional options for providing incremental capacity	In some configurations, must be used in tandem with another syngas generation technology
Two-step reforming [a]	Size of SMR is reduced	Increased process complexity
	Low methane slip favours high purity syngas applications	Higher process temperature than SMR
	Syngas methane content can be tailored by adjusting secondary reformer outlet temperature	Usually requires oxygen
ATR	Natural H_2:CO ratio often is favourable	Limited commercial experience
	Lower process temperature requirement than POX	Usually requires oxygen
	Low methane slip	
	Syngas methane content can be tailored by adjusting reformer outlet temperature	
POX	Feedstock desulfurization not required	Low natural H_2:CO ratio is a disadvantage for applications requiring ratio >2.0.
	Absence of catalyst permits carbon formation and, therefore, operation without steam, significantly lowering syngas CO content	Very high process operating temperatures
		Usually requires oxygen
	Low methane slip	High temperature heat recovery and soot formation handling adds process complexity
	Low natural H_2:CO ratio is an advantage for applications requiring ratio < 2.0	Syngas methane content is inherently low and not easily modified to meet downstream processing requirements

[a] SMR followed by oxygen-blown secondary reforming

Table 2.3: Techniques for adjusting syngas H_2:CO ratios (Karp *et al.*, 1998)

	Decreases ratio	Increases ratio
Recycle CO_2	×	
Import CO_2	×	
Remove H_2 via membrane	×	
Remove CO_2		×
Increase steam		×
Add shift converter		×

Table 2.4: Approximate variation in H_2:CO ratio for natural gas feed (Karp *et al.*, 1998)

	SMR	Two-step reforming	ATR	POX
Import CO_2 or remove H_2 via membrane	<3.0	<2.5	<1.6	<1.6
Total CO_2 recycle	3.0	2.5	1.6	1.6
No CO_2 recycle	5.0	4.0	2.65	1.8
Increase steam	>5.0	>4.0	>2.65	>1.8
Add shift converter	inf	>5.0	>3.0	>2.0

volumetric flow of gas. Questions also remain about the potential for forming ammonia and other nitrogen compounds in the downstream FT conversion units (Wilhelm *et al.*, 2001).

Also problematic with air-blown operation is the low heating value of the FT tail gas. From an economic standpoint, utilising this tail gas to generate power for export sale is a potentially key contributor to the overall viability of the GTL plant. However, combustion turbine technology and commercial experience with the use of such low quality gas remains quite limited (Wilhelm *et al.*, 2001).

2.3.2 Syngas conversion

Conversion of natural gas to Naphtha and GTL Fuel can be achieved by means of the FT process. The FT process can be operated at low temperatures (LTFT) to produce a syncrude with a large fraction of heavy, waxy hydrocarbons or it can be operated at higher temperatures (HTFT) to produce a light syncrude and olefins (Jager, 1998). Only the low temperature Fischer-Tropsch (LTFT) reactors will be discussed in this section, because we would like to operate the FT reactor at high alpha values and produce mostly heavy, waxy hydrocarbons in the GTL process. LTFT was originally performed in the

Table 2.5: Estimated cost of FischerTropsch liquid (Karp *et al.*, 1998)

Manufacturing cost % of total	
Natural gas @ US$0.50/Mscf	14.9
Operating labor	1.8
Other operating costs	19.2
Capital charges @ 20%/year	64.1
Total	100.0
Capital cost distribution	
Plant section	Percentage of total capital cost
Oxygen plant	23
Reforming	28
FischerTropsch synthesis	24
Product upgrade	13
Power recovery	12
Total	100

tubular fixed bed reactor(TFBR) (Jager & Espinoza, 1995). The TFBR is complex and expensive (Jager, 1998) and temperature control is very difficult. For this reason Sasol developed the Sasol Slurry Bed reactor (SSBR) (Jager & Espinoza, 1995). The reactor is much simpler; it is easy to operate; it has lower pressure drop; it has on-line catalyst renewal facilities and it is capable of much higher capacities (Jager & Espinoza, 1995).

Tubular fixed bed reactor (TFBR)

Fischer-tropsch synthesis in the LTFT mode was originally practised in pre-war Germany in packed beds. This developed into tubular fixed bed. Arge reactors which were commissioned at Sasol in 1955 (Jager & Espinoza, 1995).

Heat removal for the highly exothermic synthesis reaction is achieved by generation of steam on the shell side of the reactor. Earlier reactors operated at a shell side temperature of about 220°C, and a reactor pressure of 25 bar. A reactor commissioned in 1987 operated at 45 bar. The respective capacities were about 600 and 900 bbl/day per reactor. A detailed design for a 5000 tube reactor was also produced for use at the Sasolburg (South Africa) factory but eventually not used because of the development of the SSBR (Jager & Espinoza, 1995).

The products from the LTFT as obtained from the TFBR using Fe-based catalyst vary depending on the catalyst formulation and process conditions. A typical LTFT product distribution as obtained for a TFBR and that typically obtained for high temperature

Fischer-Tropsch synthesis, is given in table 2.6. The LTFT product slate follows the Schulz-Flory distribution with a typical alpha value of 0.95 (Jager & Espinoza, 1995).

Table 2.6: Selectivity of Sasol processes (Jager & Espinoza, 1995)

Product	TFBR	Synthol(fluidized bed)
CH_4	4	7
C_2 to C_4 olefins	4	24
C_2 to C_4 paraffins	4	6
Gasoline	18	36
Middle distillate	19	12
Heavy oils and waxes	148	9
Water soluble oxygentes	3	6

The reactor is complex and expensive. The scale-up of the reactor is mechanically difficult. The mechanical design is further complicated by the fact that the iron based catalyst has to be replaced periodically and the design has to provide for this. The replacement is cumbersome and maintenance and labour intensive; it causes considerable downtime and disturbances in plant operations. The product selectivities also change with aging of the catalyst. With a number of reactors the total selectivities can, however, be evened out by staggering the catalyst age in the reactors (Jager & Espinoza, 1995).

Axial and radial temperature profiles exist in the tubes, because of the exothermic nature of the Fischer-Tropsch reaction. Maximum average temperature is required for maximum conversion. This is, however, limited by the maximum allowable temperature peak that may not be exceeded in order to prevent carbon formation on the catalyst and the effect temperature has on product selectivities. Carbon formation causes breakup of the catalyst that in turn causes blockages and a need to replace the catalyst (Jager & Espinoza, 1995).

Product selectivities are temperature dependent and flexibility with respect to temperature control would be advantageous. The choice of temperature level is however severely curtailed by the need to avoid exceeding the maximum peak temperature (Jager & Espinoza, 1995).

Pressure drops across the TFBRs are high and may vary from 3 to 7 bar depending on the operating pressure. With relative high recycle flows, this gives rise to considerable recompression costs (Jager & Espinoza, 1995).

Slurry bed reactor (SBR)

Most of the difficulties of the TFBR can be eliminated in a SBR. This idea was first tried out during the Second World War and up to the late 1970's by Kölbel & Ralek (1980). Sasol's own exepriments on small scale started in the early 1980's. Although they could not repeat Kölbel's results, and it was difficult to obtain consistent results in the 5 cm diameter reactor used, they did show promise for the concept. It was realised that the hydrodynamics obtained from these small tubes is quite different from those expected from larger diameter reactors (Jager & Espinoza, 1995).

In 1990 a slurry bed with a diameter of about 1 m was commissioned which confirmed the original expectations. In June 1991, although the design issues had not all been resolved in detail, Sasol decided not to use existing designs for two 5000 tube TFBRs but rather use the slurry bed concept for its planned expansion of LTFT capacity. A single slurry bed reactor, 5 m in diameter, 22 m high, was commissioned in May 1993 and the process was called the Sasol Slurry Bed process (SSBP) (Jager & Espinoza, 1995).

The SSBR is much simpler than a TFBR, it is much easier to fabricate and is much cheaper. It consists of a shell with cooling coils in which steam is generated. Syngas is distributed in the bottom and rises through the slurry that consists of liquid reaction products, predominantly wax, with Fe-based catalyst particles suspended in it. The reagent gas diffuse from the gas bubbles through the liquid phase to the suspended catalyst where they react to produce hydrocarbons and water. The heavy hydrocarbons form part of the slurry phase whereas the lighter gaseous products with unreacted syngas pass through the freeboard above the bed and then to the gas outlet (Jager & Espinoza, 1995).

Because of the churning nature of the slurry-gas bubble interaction, the slurry phase is well mixed and tends to be isothermal. This gives much more flexible temperature control. Temperatures on average can be much higher than in a TFBR without the danger of carbon formation and break-up of catalyst. Better control of product selectivities become possible at higher average conversions. This makes it ideal for use with high activity catalysts where the problems with excessive radial and axial temperature gradients are much more pronounced (Jager & Espinoza, 1995).

The pressure drop across the bed is practically that of the static hydraulic head and is much lower than that for the TFBR. This translates to considerable savings in compression costs (Jager & Espinoza, 1995).

On-line catalyst removal and additions can be done without difficulty. This is an important improvement on the TFBR where the catalyst has to be replaced from time to

time. Losses due to down-time and labour intensive turn-arounds are eliminated (Jager & Espinoza, 1995).

It is thought possible that a single SBR with a capacity of about 10 000 bbl/day can be built. Full advantage is then taken of the potential for economy of scale (Jager & Espinoza, 1995).

2.3.3 Hydroprocessing

The current technologies in hydroprocessing will not be discussed, since only the first stage of hydroprocessing is included in this study.

2.4 Optimization of existing technologies

2.4.1 Syngas generation

Much of the forward-looking consideration of syngas production for GTL has focused on autothermal reforming. In part, this is due to the technology's basic compatibility with FT feed chemistry requirements. However, this focus also reflects the perception that ATR has other attributes-relative compactness, lower capital cost, and greater potential for economies of scale-which will contribute significantly to the economic viability of GTL plants (Wilhelm *et al.*, 2001).

Ongoing efforts to develop lower-cost syngas generation technologies include the following (Wilhelm *et al.*, 2001):

- The development and application of 'compact reformers' and of 'heat exchange reformers', in which a portion of the heat of reaction is provided by heat recovery from the reformed gas, rather than by burning fuel. Potential advantages over conventional tubular reactors include improved efficiency, smaller plant footprint, lower capital cost, and reduced emissions. Companies active in this area have included Air Products, KTI, ICI, BP/Kvaerner, Kellogg, Haldor Topsøe, Krupp Uhde, and Lurgi.
- Development and application of air-blown autothermal reformer technology, thereby eliminating the need for an oxygen plant. (Air-blown secondary reforming is well established, being commonly utilized for syngas production for ammonia plants). The chief proponent of the air-blown approach is Syntroleum.

- New reformer reactor approaches, most notably that employed by Exxon's AGC-21 process for converting natural gas to liquids. The first step in this process is syngas generation via oxygen-blown catalytic autothermal reforming in a fluidized bed reactor. The process has been demonstrated at large pilot scale of about 200 b/day.

- 'Ceramic membrane reactors', based on the use of ionic or oxygen transport membranes, which would couple air separation and partial oxidation in one unit operation, thereby eliminating the need for a conventional oxygen plant. Although being aggressively pursued by two industrial consortia, work in this area is still at a fundamental level. One consortium, led by Air Products, is being co-funded by the US Department of Energy. The participants in this effort include ARCO, Babcock and Wilcox, Chevron, Norsk Hydro and others. The second consortia, based entirely on industrial funding, involves Amoco, BP, Praxair, Statoil, Phillips Petroleum and Sasol.

According to Vosloo (2001) the thermal efficiency of the reforming section can be improved by:

1. The use of a heat exchange reformer in combination with an autothermal reformer.

2. The use of a feed/product heat exchanger to recover energy from the reformer outlet.

Heat exchange reforming

The combination of a heat exchange reformer with an ATR is very similar to combined reforming, the major difference being that the energy to the steam reformer is not supplied by a fired heater but by the exit gas from the ATR. The potential benefits of such a reforming configuration are (Vosloo, 2001):

1. Savings of about 30% in oxygen consumption.

2. An increase of about 4 percentage points in the thermal efficiency of the plant.

One of the technical issues that must be solved is the potential problem of metal dusting in the heat exchange reformer (Vosloo, 2001).

Feed/product heat exchange

The oxygen consumption can be decreased by about 3.5% and the production of liquid fuels can be increased by about 2.5% if a feed/product heat exchanger is used to preheat the natural gas to the reformer. As in the case of heat exchange reforming, metal dusting is also one of the major problems that would have to be solved (Vosloo, 2001).

These configurations highlight some of the design parameters of the syngas section that influence the cost and thermal efficiency of the GTL plant. They are as follow (Vosloo, 2001):

1. The preheat temperatures of oxygen and natural gas. The higher these temperatures are, the less oxygen will be used. The maximum preheat temperatures are determined by safety factors and by the need to prevent soot formation.

2. The pressure of steam generated in the waste heat reboiler. The higher the steam-pressure, the more efficient energy can be recovered from the steam, but the more costly the steam and boiler feed water treatment systems become. The optimum steam pressure will be determined by the relative cost of capital and energy.

2.4.2 Syngas conversion

As was already discussed under existing technologies, the slurry phase reactor is a technological breakthrough and thus the optimization of the syngas conversion process will have to look at further optimization of the catalyst. The Co catalyst can be improved as follows (Vosloo, 2001):

1. Increasing the catalyst life by making it more resistant to irreversible sulphur poisoning.

2. Changing the selectivity dependency on the H_2:CO ratio to such an extent that high diesel yields can be obtained at H_2:CO ratios similar to the usage ratio. The advantage of such a catalyst would be that, due to the increase in reaction rate at higher H_2:CO ratios, much less catalyst would be needed for the same conversion. To obtain the same conversions at a H_2:CO ratio of 1.6 than at a ratio of 2; 50% more catalyst is needed at the lower H_2:CO ratio.

2.4.3 Hydroprocessing

The optimization of existing technologies in hydroprocessing will not be discussed, since only the first stage of hydroprocessing is included in this study.

2.4.4 Integration

After an extensive search for literature on GTL process integration, it was found that not much literature was publicised on this topic. The literature that were relevant, were very secretive about what was done on integration. Hill (1998) and Vosloo (2001) gave the most information regarding this topic and the most important points were:

- Since the H_2:CO ratio of the syngas is an important design variable to maximise the production of high quality diesel, the designs of the reformer and the Fischer-Tropsch sections cannot be done in isolation. The most cost-effective design for both units can only be obtained by taking the mutual interaction between these units into account (Vosloo, 2001).

- An obvious way of improving the thermal efficiency of the process is to combine it with a power generation plant. Such a combination will create a more efficient utilization of the low pressure steam produced by the Fischer-Tropsch process (Vosloo, 2001).

- Hill (1998) also focused on the integration of the three steps together with utilities to reduce the capital cost of the GTL process. He also emphasised that heat integration is critical.

2.5 Exergy

2.5.1 The exergy concept

Thermodynamics is often used to evaluate the efficiency of a chemical process. In this evaluation, use is usually made of energy and mass balances which are based upon the first law of thermodynamics. With the first law of thermodynamics there is no difference between the quality of energy (i.e. heat or work). Thus the efficiency based upon the first law does not take different quality of energies into account (Loonen *et al.*, 2001).

To explain this in more detail, one can consider the two systems in figure 2.2. The first system has more quality of energy than the second system. The first system can still

produce work, while the second system cannot produce any work. The mass and energy in both systems are equal. Thus it can be shown that not all energy are equal (Loonen *et al.*, 2001).

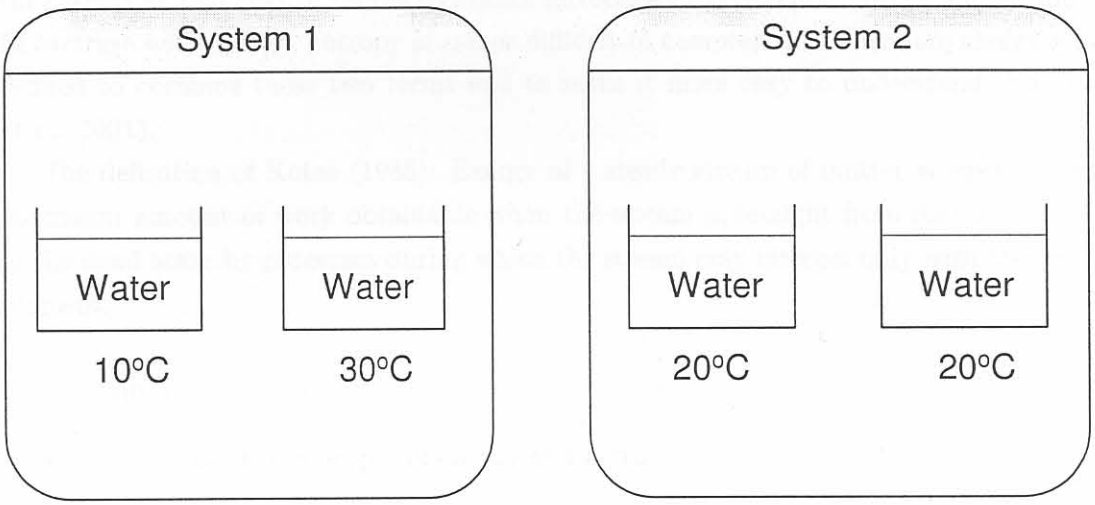

Figure 2.2: Two systems with equal energy

Except for the fact that the quality of energy and materials are not taken into account with first law thermodynamics, the internal energy losses of processes are also not taken into account. This can be seen in figure 2.3. In figure 2.3 a system is shown at three different moments in time. In this system a fuel is combusted and the combustion gases are kept within the system boundaries. Thus the total energy of the system is kept constant, but the amount of available energy to produce work decreases. This is due to the fact that the system cannot produce any work after the fuel has been combusted (Loonen *et al.*, 2001).

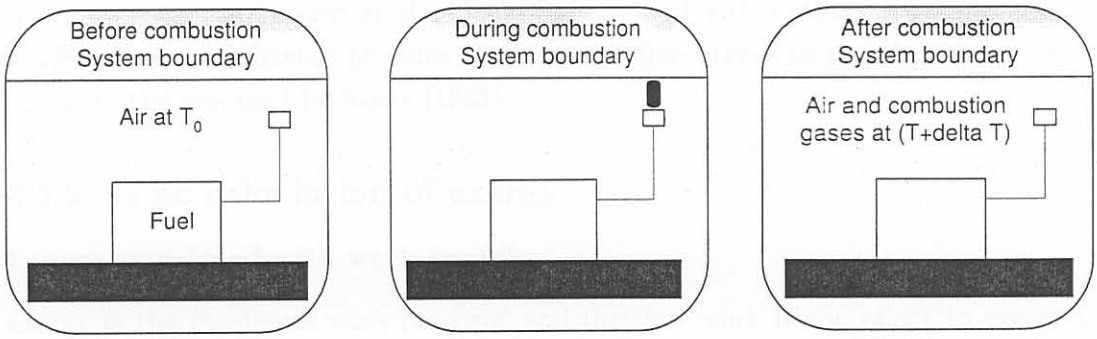

Figure 2.3: Three moments in a combustion process

It can thus be concluded that the first law of thermodynamics does not account for the quality of energy and materials. It also does not account for the internal losses of a process which would result in a higher calculated efficiency of a process than is really the case. The two laws of thermodynamics introduce two concepts: energy and entropy. In contrast with energy, entropy is rather difficult to comprehend. Therefore exergy was defined to combine these two terms and to make it more easy to understand (Loonen *et al.*, 2001).

The definition of Kotas (1985): Exergy of a steady stream of matter is equal to the maximum amount of work obtainable when the stream is brought from its initial state to the dead state by processes during which the stream may interact only with the environment.

Thus exergy is:

- derived from the concepts of energy and entropy,
- based upon the first and second laws of thermodynamics,
- referenced to the natural environment,
- a precise measure of the thermodynamic efficiency of a process.

The concept of exergy is extensively discussed in the books of Kotas (1985) and Szargut *et al.* (1988). Exergy can also be defined as the maximum work potential of a material or of a form of energy in relation to its environment that can be obtained by reversible processes. However, in reality there are only irreversible processes. For practical reasons a reference environment is considered to be so large, that its parameters are not affected by interaction with the system under consideration. In this report the reference system as stated in Szargut *et al.* (1988) has been used with a reference temperature T_0 of 298.15K and a reference pressure P_0 of 1 atm, unless otherwise stated. This system is similar to the one used by Kotas (1985).

2.5.2 The calculation of exergy

Exergy associated with work transfer

Exergy is the maximum work potential and therefore work is equivalent to exergy in every respect (Kotas, 1985). Thus exergy transfer can be specified both in magnitude

and direction by the work transfer to which it corresponds.

$$\dot{\varepsilon}^{W_x} = \dot{W}_{max} = \dot{W}_x \tag{2.7}$$

Exergy associated with heat transfer

The exergy of heat transfer at the control surface is determined from the maximum work that could be obtained from it using the environment as a reservoir of zero-grade thermal energy (Kotas, 1985). For a heat transfer rate $\dot{Q}_r$ and a temperature at the control surface where the heat transfer is taking place T_r, the maximum rate of conversion from thermal energy to work is:

$$\dot{W}_{max} = \dot{\varepsilon}^{Q} = \dot{Q}_r \tau \tag{2.8}$$

where:

$$\tau = 1 - \frac{T_0}{T_r} \tag{2.9}$$

τ is called the dimensionless exergetic temperature and is equal to the Carnot efficiency for the special case when the environment, at temperature T_0, is used as the other thermal energy reservoir. The exergy associated with a heat transfer rate is called thermal exergy flow and is denoted in open system analysis, by $\dot{\varepsilon}^{Q}$.

Exergy associated with a steady stream of matter

As with energy, exergy of a stream of matter, $\dot{\varepsilon}$, can be divided into distinct components. In the absence of nuclear effects, magnetism, electricity and surface tension, $\dot{\varepsilon}$ is:

$$\dot{\varepsilon} = \dot{\varepsilon}_k + \dot{\varepsilon}p + \dot{\varepsilon}_{ph} + \dot{\varepsilon}_0 \tag{2.10}$$

$\dot{\varepsilon}_k$ and $\dot{\varepsilon}_p$ are associated with high grade energy and $\dot{\varepsilon}_{ph}$ and $\dot{\varepsilon}_0$ with low grade energy (Kotas, 1985). The kinetic and potential energies of a stream of substance are ordered forms of energy and thus fully convertible to work. Therefor, when evaluated in relation to the environmental reference datum levels, they are equal to kinetic and potential energy respectively. Thus:

$$\dot{\varepsilon}_k = \dot{m}\frac{C_0^2}{2} \tag{2.11}$$

$$\dot{\varepsilon}_p = \dot{m} g_E Z_0 \tag{2.12}$$

where $\dot{m}$ is the mass flow rate of the fluid stream, C_0 bulk velocity of the fluid stream relative to the surface of the earth, Z_0 altitude of the stream above the sea level, and g_E gravitational acceleration (specific gravitational force), considered a constant (Kotas, 1985).

In most cases the kinetic and potential exergy can be ignored when compared with the chemical and physical components (Loonen *et al.*, 2001). It is convenient to separate physical exergy $\dot{\varepsilon}_{ph}$ and chemical exergy $\dot{\varepsilon}_0$, enabling calculation of exergy values using standard chemical exergy tables which can be found in Kotas (1985).

Physical exergy is equal to the maximum amount of work obtainable when the stream of substances is brought from its initial state to the environmental state defined by P_0 and T_0 by physical processes involving only thermal interaction with the environment (Kotas, 1985)

The physical component can be derived from the first and second laws of thermodynamics. The first law states that:

$$(H_0 - H_1) = Q_0 + W_x \tag{2.13}$$

and the maximum work potential exist when the entropy production is equal to 0 and then according to the second law:

$$\Pi = 0 = (S_0 - S_1) - \frac{Q_0}{T} \tag{2.14}$$

When equation 2.13 and equation 2.14 are combined, we get the physical component that resembles the maximum work potential (Kotas, 1985):

$$\varepsilon_{ph} \equiv (H - H_0) - T_0(S - S_0) \tag{2.15}$$

The physical component consists of a temperature and pressure dependent component (Kotas, 1985):

$$\varepsilon_{ph} = \varepsilon^{\Delta T} + \varepsilon^{\Delta P} \tag{2.16}$$

The temperature dependent component of the physical component, also known as the thermal exergy component, can be calculated as follows (Kotas, 1985):

$$\varepsilon^{\Delta T} = \int_{T_0}^{T} C_p dT - T_0 \int_{T_0}^{T} \frac{C_p}{T} dT \tag{2.17}$$

The chemical exergy is equal to the minimum amount of work obtainable when the substance under consideration is brought from the environmental state to the dead state by processes involving heat transfer and exchange of substances only with the environment (Kotas, 1985).

To assess the work potential (i.e. exergy) of a stream of substance by virtue of the difference between its chemical potential and that of the environment, the properties of the chemical elements comprising the stream must be referred to the properties of some corresponding suitably selected substances in the environment. One essential characteristic of these reference substances is that they must be in equilibrium with the rest of the environment. A table of these standard chemical exergies can be found in Kotas (1985).

In many important applications the working medium consists of a mixture of ideal gases, for example gaseous fuels, combustion products, etc. The expression for the chemical exergy of mixtures is:

$$\varepsilon_0 = \sum_i x_i \varepsilon_{0,i} + RT \sum_i x_i \ln x_i \tag{2.18}$$

Since the second term on the right hand side is always negative, the exergy of the mixture is always less than the sum of the exergies of the components at the pressure and temperature of the mixture.

2.6 Efficiency

2.6.1 Exergetic efficiency

Exergy efficiency and irreversibilty should be used as a measure for the total resource efficiency (van Schijndel *et al.*, 2001). The efficiency of a process can be calculated in various ways by the use of the principles of thermodynamics. Traditionally the efficiency was calculated by means of mass and energy balances. But these efficiencies could not indicate the real quality of the processes. A process should be evaluated according to the second law of thermodynamics to take the quality of energy into account. This quality of energy then describes the efficiency of the process relative to the maximum work obtainable from the process. This is called exergy and takes into account the first law (energy) and second law (entropy) of thermodynamics. An exergy analysis describes all losses, internal and external to the process.

An exergy analysis describes both internal and external process losses. Internal losses,

also called irreversibilities, take place due to internal degradation of energy, while external losses can occur if process streams are emitted into the environment.

Equation 2.19 describes the exergy balance and it is also illustrated in figure 2.4.

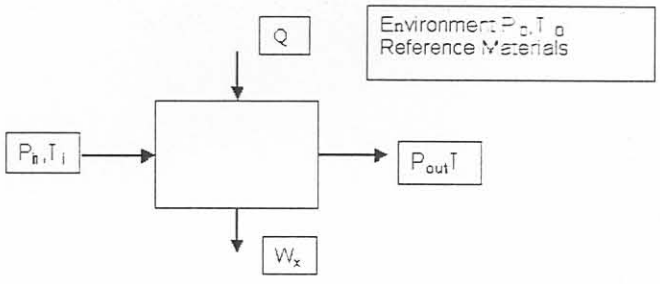

Figure 2.4: The defined system for exergy analysis

$$\dot{\varepsilon}_{in} + \dot{\varepsilon}^{Q} = \dot{\varepsilon}^{W_x} + \dot{\varepsilon}_{out} + \dot{I} \tag{2.19}$$

Variable	Description
$\dot{\varepsilon}_{in}, \dot{\varepsilon}_{out}$	in and out going exergy material streams
$\dot{\varepsilon}^{Q}$	exergy heat stream
$\dot{\varepsilon}^{W_x}$	exergy work stream
$\dot{I}$	irreversibility $= T_0 \cdot \Pi$ where Π = entropy production

Irreversibilities are loss of exergy. Loss of exergy means loss of work potential. Lost work potential then has to be generated somewhere else in the process. This normally results in the use of primary fuel. Minimizing exergy losses is thus directly equivalent to saving primary fuel.

In this study Exercom was used to evaluate all the exergy values from the Aspen Plus model. Exercom is an add-on module to Aspen Plus.

2.6.2 Carbon efficiency

To examine the exergy and stoichiometry limitations of hydrocarbon production; targets have to be determined. In this study carbon efficiency (defined as the amount of carbon in the process that ends up in hydrocarbon products) and exergy efficiency (which is discussed in the exergy section) has been used as the main targets. A carbon efficiency

lower than 100% implies that carbon has to leave the system as CO_2. A carbon efficiency of higher than 100% implies that CO_2 can be used as a feed to the system.

Chapter 3

Process design

3.1 Process design objectives

The design objectives of the GTL process were:

- optimization of product yield (i.e. maximum carbon efficiency) and
- minimum energy requirements.

To obtain these objectives, various process configurations and technologies were considered of which the background is given in chapter 2.

3.2 Assumptions

The following assumptions were made for this study:

- When referring to the GTL process, only the Fischer-Tropsch reactor and the reformer are taken into account for integration purposes. The integration of the hydroprocessing unit was not considered.
- High quality natural gas (95% methane) was used as feedstock.
- All import power and heat that is not generated within the process itself has a generation exergetic efficiency of 50% (thus a penalty).
- Maximum preheating of the reformer feed with the reformer product ($\Delta T = 75°C$) could be done in heat exchangers without sooting or metal dusting problems.

- The Fischer–Tropsch reactor model did not include a trade-off between a decrease in selectivity and an increase in reaction rate for a higher H_2:CO ratio.

3.3 Process description

To make the following discussion easier to follow, a schematic diagram of the final process design can be seen in figure 3.1. This design is the result of the discussion in this chapter.

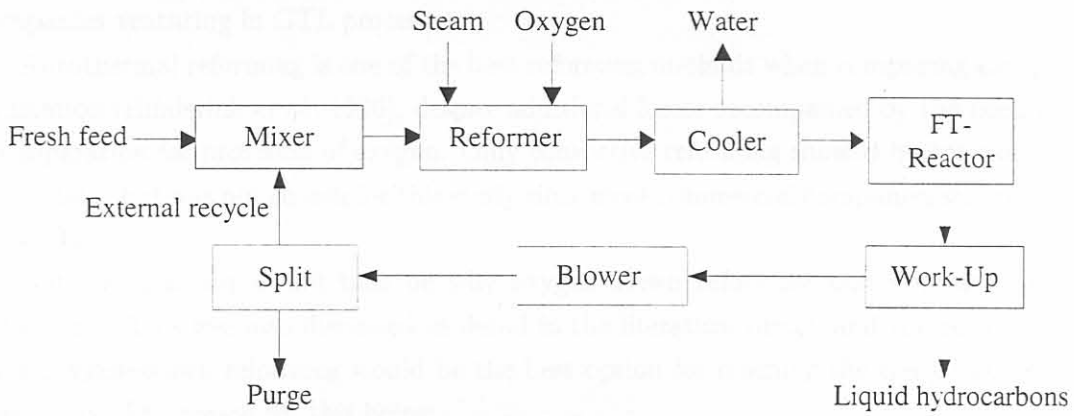

Figure 3.1: The final design of the GTL process (without integration)

3.3.1 Overall layout

It can be seen from figure 3.1 that the external recycle is mixed with the fresh natural gas feed to form the total feed to the reformer. Steam and oxygen is also added to the reformer to obtain the correct H_2:CO ratio in the synthesis gas (product of the reformer). The synthesis gas is then cooled with utilities to separate most of the water from the FT feed to protect the cobalt catalyst in the FT reactor. Once the synthesis gas has been converted to liquid hydrocarbons in the FT reactor, it is fed to the work–up unit to separate the liquid hydrocarbons from the light gases. These light gases consist of unreacted H_2 and CO, and CO_2, methane, ethane, propane and butane. The maximum amount of gas is recycled (externally) to the reformer to obtain the desired H_2:CO ratio in the synthesis gas. This is done by purging the minimum amount of gas. The maximum amount of external recycle (i.e. maximum amount of CO_2 recycle) is used to control the H_2:CO ratio in the synthesis gas together with the steam and oxygen feed to the reformer.

The only other manipulated variable to control the H_2:CO ratio in the synthesis gas is the temperature of the reformer.

3.3.2 The reformer

FT synthesis calls for a H_2:CO ratio of about 2, a value higher than that achievable with partial oxidation and lower than that obtainable with SMR. Autothermal reforming (ATR) combines partial oxidation with catalytic steam reforming in one reactor. For this reason the ATR was chosen since it is generally the choice for all the commercial companies venturing in GTL processes.

Autothermal reforming is one of the best reforming methods when comparing exergy-utilization (Hinderink *et al.*, 1996), despite additional losses accompanied by the need for air separation for provision of oxygen. Only convective reforming showed better exergy-utilization, but was not chosen for this study since most commercial companies still invest in ATRs.

But the question would thus be why oxygen–blown reforming and not air–blown reforming? This was also discussed in detail in the literature survey and the result was that oxygen–blown reforming would be the best option for reaching the design goals in this study. The reason for this being:

1. external recycling of the Fischer-Tropsch tailgas is only possible with oxygen-blown reforming,

2. only with recycling of the Fischer-Tropsch tailgas will maximum carbon efficiency and maximum product yield be reached and

3. the Fischer-Tropsch tailgas has a higher energy density value, thus it could be utilised for generating power which could be the contributor to viability of the GTL plant.

Jager (1998) also discussed the importance of economy of scale for this process. The major cost of the GTL process is the production of syngas. A major part of this cost is the cost of oxygen, which is sensitive to economy of scale. Therefore the assumption will be made for this study that the process will be done on large scale.

Another point made by Jager (1998) and Vosloo (2001) is that much research and development are being done on oxygen separation membranes. But this technology is also not suited for large scale operations and was thus not considered.

Autothermal reforming (ATR) was used in this process to reform the large amount of methane in the natural gas. The ATR reforms enough methane to produce a H_2:CO ratio of 2.15 which is the ratio needed for a Schulz–Flory alpha value of 0.95 in the Fischer-Tropsch reactor (see appendix B). The minimum amount of steam and oxygen were added to the reformer feed, because it has a positive impact on both product-gas composition and investment and operating costs of the reformer (Ernst *et al.*, 2000).

This means that one would like to work at the lowest possible H_2O/C ratio in the ATR that would be practical. Haldor Topsø and Sasol did some work on this issue and have successfully run an ATR with a S/C ratio of 0.6 with a reactor exit temperature of 1050°C (Ernst *et al.*, 2000). This was a major achievement, since the usual S/C ratios were 1.7–2.2 for the ATR.

These high ratios were necessary because (when the ATR is operated at a low S/C ratio) the following might occur (Ernst *et al.*, 2000):

1. Tendency for sooting increases
2. Syngas composition changes
3. Potential for metal-dusting corrosion increases

All carbon gases that are fed to the reformer are reformed and thus contribute to improving the H_2:CO ratio in the feed to the reactor. The reforming reaction (equation 3.1) with the accompanied water gas shift (WGS) reaction (equation 3.2) is as follows:

$$C_nH_{2n+2} + nH_2O \rightarrow nCO + (2n+1)H_2, \qquad \Delta_rH^0 = 206.3\frac{kJ}{molCH_4} \tag{3.1}$$

$$CO + H_2O \rightleftharpoons CO_2 + H_2, \qquad \Delta_rH^0 = -40.6\frac{kJ}{mol} \tag{3.2}$$

Starting from methane (n=1) as feed for the reforming, a synthesis gas can be obtained by reaction equation 3.1 which has a stoichiometric H_2:CO molar ratio of (2n+1)/n = 3. But reforming also takes place by CH_4 reacting with CO_2 (equation 3.3) giving a stoichiometric H_2:CO molar ratio of 1.

$$CH_4 + CO_2 \rightleftharpoons 2CO + 2H_2, \qquad \Delta_rH^0 = 246.9\frac{kJ}{mol} \tag{3.3}$$

Thus we can achieve the target H_2:CO molar ratio of 2.15 by combining these reactions.

But where do we get the extra CO_2 to decrease the syngas H_2:CO ratio? Various options exist for CO_2 recycling to the ATR. In conventional practice, the carbon dioxide is obtained by separation of CO_2 from the reformer output and recycled back to the ATR. But separation of CO_2 is often carried out by amine stripping which is very expensive. Thus it would be advantageous not to have the CO_2 removal step. But CO_2 recycling to the ATR could still be accomplished by recycling Fischer-Tropsch tailgas (which is CO_2 rich) to the ATR.

Three recycling options exist:

- internal CO_2 recycling over reformer,
- internal Fischer-Tropsch tailgas recycling over Fischer-Tropsch reactor and
- external Fischer-Tropsch tailgas recycling to ATR.

The first recycling option would entail a special CO_2 recovery unit after the ATR and thus major investment costs. This option was not considered.

The second recycling option would entail recycling of Fischer-Tropsch tailgas after the product separation step back to the SBR to increase the conversion in the reactor. But since the SBR was chosen (80% conversion) it was decided that the conversion would be high enough not to do internal recycling. The high conversion in the Fischer-Tropsch reactor is necessary to prevent an enormous recycle stream that would increase capital costs with large processing units. Internal recycling would also entail compression costs.

The third recycling option seemed to be the best option to attain maximum product yield (i.e. maximum carbon efficiency). CO_2 would be recycled to the ATR to control the syngas H_2:CO ratio and improve the carbon efficiency without having extra equipment for CO_2 separation.

The principal partial oxidation reaction that supplies the heat for the other endothermic reactions (equation 3.1 and equation 3.3) is:

$$CH_4 + \frac{1}{2}O_2 \rightarrow CO + 2H_2, \qquad \Delta_r H^0 = -35.6\frac{kJ}{mol} \tag{3.4}$$

The temperature in the reformer affects the extent of both the reforming and the WGS reaction in the reformer. In this study various case scenarios were considered with temperatures ranging between 850°C and 1170°C to find the optimum temperature of the ATR to satisfy the design goals.

3.3.3 The low temperature Fischer-Tropsch reactor

Since this study was done with the focus on developments especially in South Africa with Sasol being a world leader in Fischer-Tropsch synthesis, it was decided that the low temperature Fischer-Tropsch Slurry Bed Reactor (SBR) would be used in the process. This was done because of the following reasons:

1. A 10 000 bbl/day SBR is possible and can thus take full advantage of economy of scale,

2. the technical advantages of the SBR over the TFBR (Jager, 1998), i.e. higher average conversions, better product selectivities, lower pressure drop, on–line catalyst removal and more flexible temperature control and

3. the SBR is easier to fabricate and cheaper than the TFBR (Jager, 1998).

After the reforming has been done, the water has to be separated from the FT feed to prevent catalyst deactivation in the SBR. Refer to the literature survey on the influence of CO_2 and H_2O on the Fischer-Tropsch synthesis. Although it is accepted that water or carbon dioxide do not have an inhibiting effect on the rate of FT synthesis for cobalt catalysts, a certain degree of oxidation does still take place with water present in the feed (Espinoza *et al.*, 1999). Therefore it was decided that water should be removed after the ATR to prolong the life of the cobalt catalyst.

The Slurry Bed Reactor (SBR) is used to convert the synthesis gas to liquid fuels and waxes through Fischer-Tropsch synthesis. It was assumed that only the cobalt catalyst will be used and thus negligible WGS will occur. The reactor conditions are 23 bar and 260°C. These conditions were chosen to promote a high alpha value of 0.95 (according to the Schulz-Flory distribution) for the production of liquid fuels and waxes, rather than fuel gas and LPG. Therefore the specific syngas H_2:CO consumption ratio is 2.15 (refer to appendix B for the precise calculation of the H_2:CO consumption ratio).

In practice, the growth probability alpha depends on temperature, catalyst, reactor type and partial pressures of hydrogen and carbon monoxide. For low-temperature Fischer-Tropsch (200-260°C), alpha values between 0.85–0.95 are achieved. This corresponds to a H_2:CO consumption ratio of 2.335–2.158.

Equation 2.6 was used to determine alpha for this study.

Only the production of paraffins was considered in this study, neglecting the production of olefins and oxygenates. Thus no selectivity model was introduced for selection

between paraffins, olefins and oxygenates. The Schulz–Flory model was used for predicting the selectivity of the paraffin distribution.

Although equation 2.6 was based on experiments using a precipitated iron catalyst that also catalyses the WGS reaction (equation 2.3), it is believed that industrial cobalt catalysts show similar selectivities without catalysing the WGS reaction (Lox & Froment, 1993). The equation reflects that selectivity increases with carbon monoxide partial pressure, and decreases with hydrogen partial pressure.

Predicted alpha values at FT conditions of 260°C, 20 bar and 80% conversion are 0.946-0.956 for undiluted synthesis gas (H_2:CO ratio of 2). The higher values correspond to a reactor with the liquid in plug flow (e.g. a fixed bed, multi-tubular reactor) while the lower values correspond to a reactor in which the liquid is well mixed (e.g. a slurry reactor). The lower values were used for this work. The FT temperature was fixed at 260°C because equation 2.6 predicts rather optimistic values at lower temperatures.

The conversion in the reactor also plays an important role in the total H_2:CO molar ratio in the loop and was set at 80% (Espinoza *et al.*, 1999).

3.3.4 Work-Up

The heavy oil and liquid fuel fractions are separated from the light gases with the separation column. This separation column resembles a combined heavy oil separation drum (C_{12+}) and a light oil (C_{5-11}) and water distillation column. The operating conditions of the separation column are set at the Fischer-Tropsch reactor operating conditions (23 bar and 260°C). The two units that are represented in this single separation model are discussed in the following 2 sections:

The heavy oil separation drum

The heavy oil fractions are separated with the flash drum. The operating conditions of the flash drum are set at the Fischer-Tropsch reactor operating conditions. The overhead gases are sent to the light oil and water distillation column.

The light oil and water distillation column

The distillation column is operated with only a condenser. All the feed enters the column as a gas feed at the lowest stage (which is stage 5). The top stage temperature is held at 40°C with the bottom stage at 178°C. Separation was done with the aim to recycle methane, ethane, propane and butane.

The light gases (H_2, CO,CO_2, CH_4, C_2H_6, C_3H_8 and C_4H_{10}) exit the separation column as feed to the recycle loop.

3.3.5 Other process units

The natural gas is received at a pressure of 60 bar and isenthalpically depressurised to 26 bar. Between the reformer and the low temperature Fischer-Tropsch reactor the process stream is cooled down to remove the excess water. The reason for this is that excess water will deactivate the cobalt catalyst at a much higher rate. After work-up there is a blower to bring the recycle back to process pressure of 26 bar.

3.4 Process integration

See figure 3.2 for the following discussion. This section discusses the final result of the integration process. Before any exergy analysis could be done, thorough consideration had to be given to all the utilities used in the recycle process. Any inefficiency in producing the utilities had to be transparent in the efficiency of the recycle process. The heat integration was focused on recovering heat from the Fischer-Tropsch reactor, from the reformer and from the purge stream.

3.4.1 Import heat and power

Any power or heat that was not generated with integration within the GTL process boundaries and had to be imported. was assumed to have been generated with certain exergy efficiencies (Kerkhof & van Steenderen, 2000):

- Power (electricity) for driving compressors is generated with an exergetic efficiency of 50%.
- Import heat exergy is generated with an exergetic efficiency of 50%.

3.4.2 Recovering heat from the Fischer-Tropsch reactor

The heat from the exothermic Fischer-Tropsch reactions is used to generate saturated steam at 24 bar. The water is initially at environmental temperature and pressure and is then pumped to a pressure of 24 bar. The pressurised water is then vapourised with the heat from the Fischer-Tropsch reactor to a temperature of 222°C.

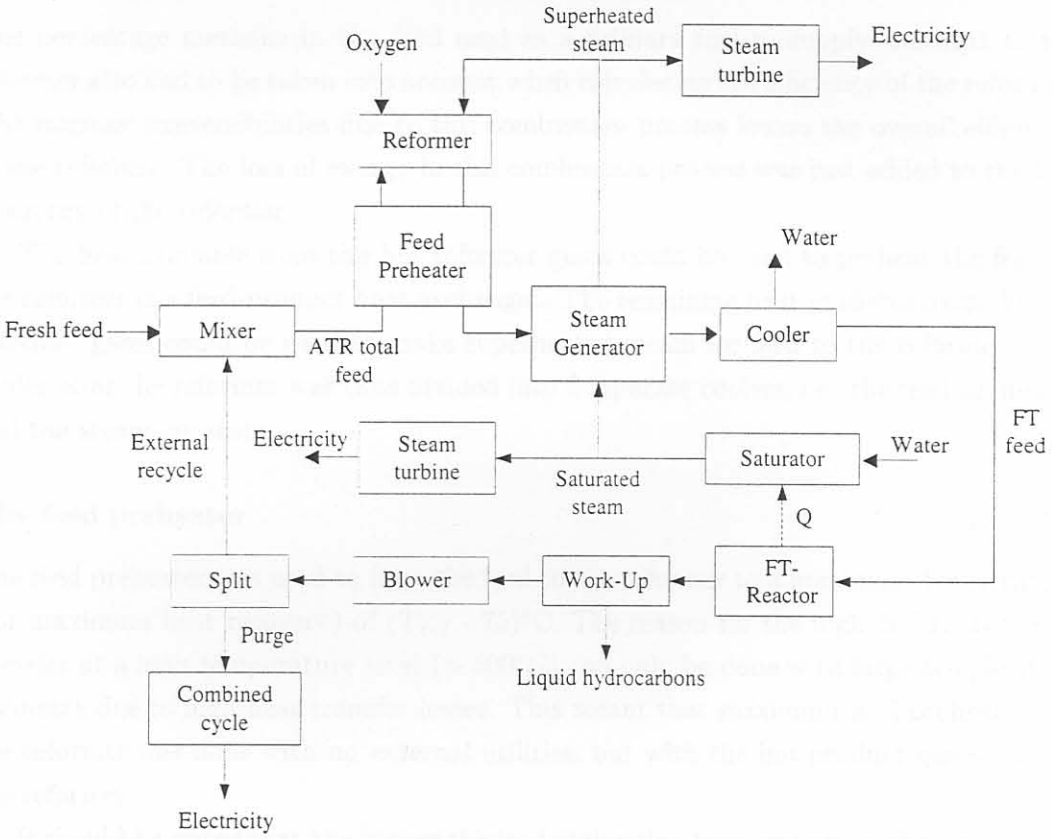

Figure 3.2: The final design of the GTL process with process integration

The saturated steam is then sent to the steam generator to be heated to 430°C. If more saturated steam is made than is necessary for the steam generator, then the saturated steam is sent through a steam turbine to generate electricity (exergy efficiency = 70%). The electricity can then be used in the process for driving pumps and blowers to improve the overall exergetic efficiency of the GTL process.

3.4.3 Recovering heat from the reformer

The percentage methane in the feed used as a primary fuel to supply the heat to the reformer also had to be taken into account when calculating the efficiency of the reformer. The intrinsic irreversibilities due to this combustion process lowers the overall efficiency of the reformer. The loss of exergy in this combustion process was just added to the loss of exergy of the reformer.

The heat available from the hot reformer gases could be used to preheat the feed to the reformer in a feed-product heat exchanger. The remaining heat available from the hot reformer gases could be used to make superheated steam for feed to the reformer. The cooler after the reformer was thus divided into 2 separate coolers, i.e. the feed preheater and the steam generator.

The feed preheater

The feed preheater was used to heat the feed to the reformer to a maximum temperature (for maximum heat recovery) of (T_{ref} - 75)°C. The reason for the high ΔT is that heat transfer at a high temperature level ($> 600°C$) can only be done with large temperature gradients due to high heat transfer losses. This meant that maximum feed preheating to the reformer was done with no external utilities, but with the hot product gases exiting the reformer.

It should be noted that the higher the feed preheating temperature is, the less oxygen will be used. It was also assumed that no sooting or metal dusting problems will occur in this heat exchanger.

The steam generator

The second heat exchanger heats saturated steam at 24 bar to the required superheated steam for the reformer at 24 bar and 430°C. Depending on the temperature of the reformer, enough heat is available for creating even more steam than necessary for the reformer. The extra heat is then used to produce superheated steam which can be used

in a steam turbine to generate electricity (exergy efficiency = 70%). The electricity can then be used in the process for driving pumps and blowers to improve the overall exergetic efficiency of the GTL process.

3.4.4 Recovering heat from the purge stream

The purge stream is necessary, because if too much CO_2 is recycled to the reformer, then the H_2:CO ratio of the syngas becomes too low to obtain an alpha value of 0.95 in the Fischer-Tropsch reactor. The design goals were to maximise the product yield and carbon efficiency of the GTL process. This could only be done by recycling the maximum amount of CO_2, unconverted CO, CH_4, C_2H_6, C_3H_8 and C_4H_{10} back to the reformer while maintaining the H_2:CO ratio of 2.15 for the syngas.

One of the other objectives of the process design was to minimise energy requirements for the process. Therefore the purge stream was evaluated as a stream which could be used for electricity generation, because of its high heating value. The best option to convert the gas to electricity is with the combined cycle. With the combined cycle the purge gas is incinerated in a gas turbine, and steam is generated from the hot gas turbine exhaust gases for additional electricity generation in a steam turbine. The combined cycle has an exergy efficiency of 50% (Williams & Larson, 1993). The steam–Rankine cycle and the steam injected gas turbine were also considered, but their efficiencies are lower than the combined cycle and was discarded.

Chapter 4

Process modelling using Aspen Plus software

Refer again to figure 3.2 for the following discussion.

4.1 The natural gas feedstock

A typical natural gas composition was used for all the simulations. The methane content is that of high quality natural gas (see table 4.1).

Table 4.1: Natural gas composition for GTL study

Component	Mole %
CH_4	94.8%
C_2H_6	2.6%
C_3H_8	0.2%
C_4H_{10}	0.03%
C_5H_{12}	0.01%
C_6H_{14}	0.01%
N_2	1.6%
CO_2	0.81%
O_2	0.02%

This composition is common to the natural gas found in the Union Gas system in North America (Union-Gas, May 2002).

4.2 The reformer

The autothermal reformer is modelled by the Gibbs reactor model in Aspen Plus. This reactor model calculates the product compositions from the reactor by minimising the total free Gibbs energy. The reforming (refer to equations 2.1 and 2.2) as well as the water gas shift reaction (refer to equation 2.3) are thus taken into account, without specifying the necessary reaction equations. Therefore there is no need to change the reformer model if a separation change is made in the light oil and water distillation column. This is very handy for when the recycle loop is closed and the range of hydrocarbons being reformed changes with every iteration. The reformer pressure was specified at 24 bar and the temperature was varied between 850°C and 1170°C to find the optimum temperature to satisfy the design goals.

4.3 Feed preheater

The feed preheater supplies the maximum preheating to the hydrocarbon feed. The stream is heated from 160°C to (T_{ref} - 75)°C. The two stream heat exchanger model was used in Aspen Plus with a design constraint on the outlet temperature of the cold stream at (T_{ref} - 75)°C. It was assumed that the high preheat temperatures would not cause soot formation or metal dusting in the heat exchanger.

4.4 The steam generator

The steam generator is also modelled with the two stream heat exchanger model in Aspen Plus. Saturated water at 24 bar are heated to superheated steam by the reformer tailgas. The design constraint of 430°C was put on the cold stream outlet temperature. This results in saturated water being heated from 222°C to 430°C which is superheated steam at the correct temperature and pressure for feed to the reformer.

The saturated water is obtained from environmental water (pumped to 24 bar) which has been saturated with heat from the exothermic Fischer–Tropsch reaction. Depending on the temperature of the reformer, extra superheated steam needs to be imported for feed to the reformer or surplus superheated steam can be exported. The exported steam is converted to electricity in a steam turbine and used in the GTL process for pumps and blowers.

4.5 Water separation

Although cooling of the syngas has already taken place with the two heat exchangers, further cooling to 50°C is done to condense out any excess water which could deactivate the cobalt catalyst in the Fischer–Tropsch reactor. The syngas is then heated again to 260°C (with imported heat) to minimise any exergy losses in the FT reactor because of mixing irreversibilities.

4.6 The low temperature Fischer-Tropsch reactor

The slurry phase Fischer-Tropsch reactor (rstoic) was modelled according to the reactions taking place in the reactor with the assumption that olefin production will not be modelled. The alkane reactions for the production of C_1 to C_{24} were modelled by the 'rstoic' model in Aspen Plus. The reaction modelled for these components was the following:

$$nCO + (2n+1)H_2 \rightarrow C_nH_{2n+2} + nH_2O \tag{4.1}$$

The conversion of each of these reactions were calculated according to the Anderson-Schulz-Flory distribution. For this distribution, the probability of chain growth is given. See also chapter 2. This probability is a value between 0 and 1. The higher the value, the higher the probability of high carbon chain growth and thus more waxes. For this simulation a CO conversion of 80% was assumed (Espinoza *et al.*, 1999). The reactor temperature and pressure were 260°C and 23 bar. A pressure decrease of 1 bar was assumed. The Fischer–Tropsch reactions are very exothermic. Cooling is done by water at 24 bar in a cooling coil inside the reactor. The water is then saturated and used as feed for the steam generator.

4.7 The separation column

The separation column (Sep block) was modelled as a simplification of both the heavy oil separation drum and the light oil and water distillation column. This was done as to minimise convergence problems with separation as the composition of the recycle changes with every iteration.

With the separation block it was assumed that all water could be removed from the light gases exiting the separation column. The other assumptions were that all methane

could be separated and recycled into the loop.

4.8 The condenser (modelled separate because of the Sep block)

The condenser was modelled as a cooler to cool the product gas from the separation column to 40 °C as would have automatically happened if the light oil and distillation column would have been modelled with the Radfrac model. This must be done for the exergy analysis, because the purge stream has to be at the lowest possible temperature.

4.9 The blower

The blower was modelled by the Aspen Plus compressor model with a specified discharge pressure. The tailgas is compressed to 26 bar to reduce any pressure exergy losses when mixing occurs with the fresh feed at 26 bar.

4.10 The purge

A split block introduced the purge stream. Depending on the temperature of the reformer, the purge was always varied to obtain maximum recycling for the syngas to the Fischer–Tropsch reactor to reach a H_2:CO ratio of 2.15. As already mentioned, this specific ratio is necessary to stay in a specific product range in the Fischer–Tropsch reactor.

The purged stream has high heating value and can therefore be converted to electricity to maintain a high exergetic efficiency for the whole process. This is done by a combined cycle. With the combined cycle the purge gas is incinerated in a gas turbine, and steam is generated from the hot gas turbine exhaust gases for additional electricity generation in a steam turbine. The combined cycle has an exergy efficiency of 50%.

Chapter 5

Results and discussion

5.1 The process synthesis study to determine the governing interaction variables of the process

The process synthesis study on the GTL process was done to find the governing interaction variables of the combined reforming and FT processes (with external recycle). The results of the process synthesis study was used to construct the basic process layout.

The simulation used in this section was discussed in the design chapter (chapter 3) and for this section no process integration was used. The reason for this is that the integration complicates the interaction between the units. To determine the governing interaction variables in order to improve our basic understanding of the GTL process, the process was studied in its simplest form.

5.1.1 Controlling the H_2:CO ratio of the syngas

At the exit of the reformer, the syngas (product from the reformer) will be the equilibrium of the methane reforming and the water gas shift reactions (see equations 3.1 and 3.2). Equilibrium thermodynamics determine syngas composition by the adiabatic heat balance. Main variables are exit pressure and feed ratios: H_2O/C, CO_2/C and O_2/C. Reformer temperature is directly linked to O_2/C feed ratio. The equilibrium simulation results can be seen in figure 5.1 and 5.2.

Figure 5.1 shows the simulation results of the syngas ratio and oxygen consumption dependence of the H_2O/CH_4 feed ratio. The temperature in the reformer is dependent on the amount of oxygen fed, thus the temperature varied accordingly between 900°C and 1200°C.

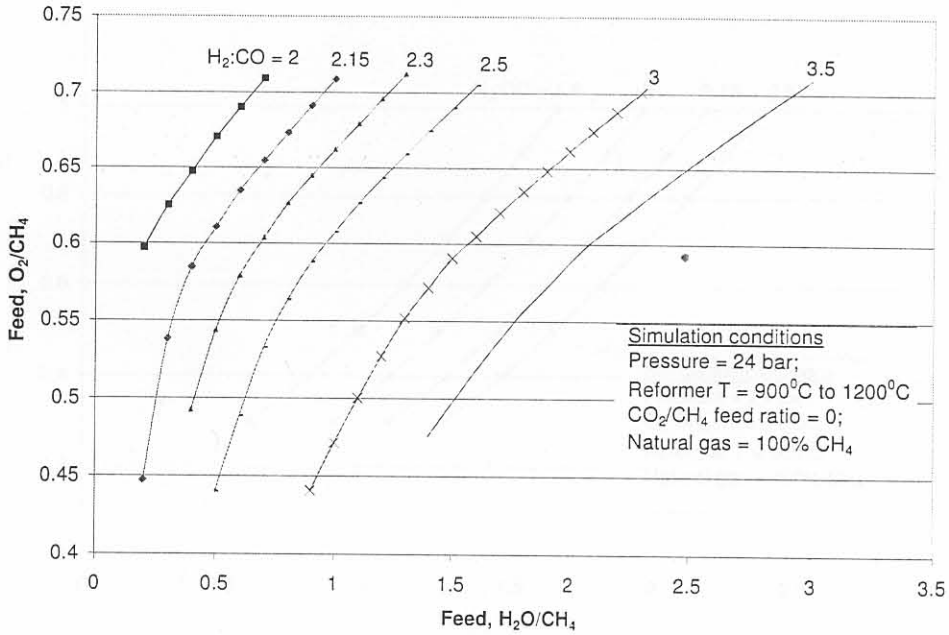

Figure 5.1: The H_2:CO ratios of the syngas without CO_2 feed

Traditionally, ATR plants operate at H_2O/C ratios of 2.0 to 3.5 yielding H_2:CO ratios of between 3.3 and 4.0 (Christensen & Primdahl, 1994). Production of H_2/CO ratio below 2.2 requires CO_2 addition. The effect of adding (recycle or import) CO_2 is illustrated in figure 5.2, which shows that curves for constant H_2:CO ratios are dependent on two feed ratios: H_2O/C and CO_2/C.

The most important curve for our study is the constant H_2:CO ratio curve of 2.15. To obtain maximum carbon efficiency, maximum CO_2 recycle is required while maintaining a H_2:CO syngas ratio of 2.15. This temperature is a function of the O_2/CH_4 feed ratio. Thus the optimum temperature of the reformer needs to be targetted, because the temperature in the reformer would determine the maximum amount of CO_2 which could be recycled and also the success of integration that could take place between the process units.

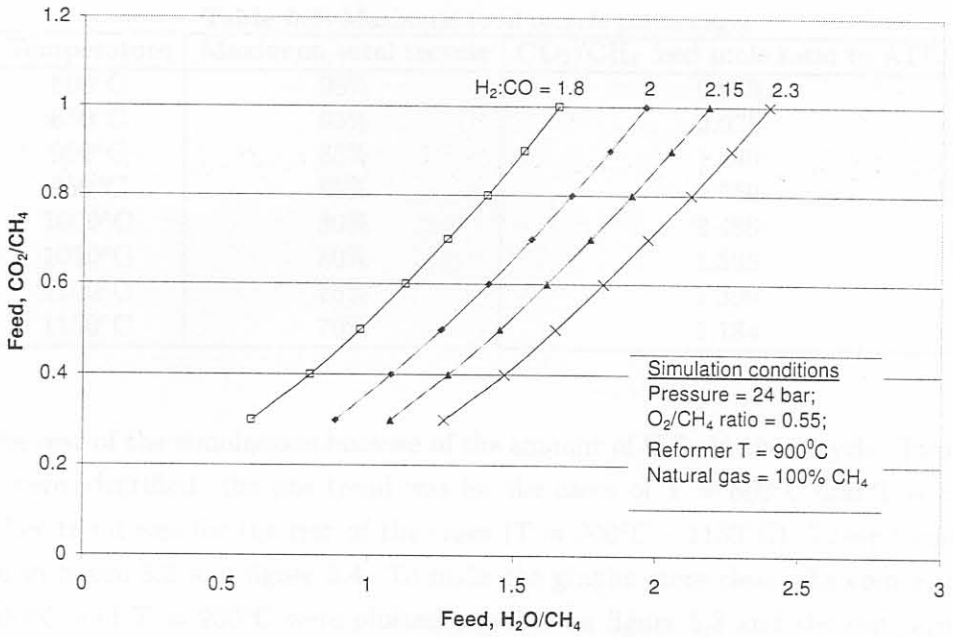

Figure 5.2: The H_2:CO ratios of the syngas with CO_2 feed

5.1.2 Varying ATR temperature with maximum amount of CO_2 recycling

An Aspen Plus simulation was used for varying the ATR temperature between 800°C and 1150°C with intervals of 50°C. The O_2/C feed ratio was manipulated to a minimum to maintain the specific temperature. The H_2O/C feed ratio was also manipulated to a minimum to maintain a H_2:CO syngas ratio of 2.15. Taking all the said conditions into account, the external recycle was varied between 0 and maximum. Maximum external recycle flow is reached when it is impossible to maintain a H_2:CO syngas ratio of 2.15, because the CO_2 in the external recycle lowers the H_2:CO syngas ratio. In other words there exists a maximum recycle capability for every specific ATR temperature with the other manipulated variables (O_2/C and H_2O/C feed ratios) at a minimum.

The maximum total recycle percentages that were achieved can be seen in table 5.1 as well as the maximum amount of CO_2 recycled given as a fraction of the total amount of CH_4 fed to the reformer.

A total recycle of 95% implies that 95% of the work–up tailgas is recycled and 5% is purged. From table 5.1 it can be seen that the simulations at 800 and 850°C differ

Table 5.1: Maximum total recycle percentages

Temperature	Maximum total recycle	CO_2/CH_4 feed mole ratio to ATR
800°C	95%	0.069
850°C	95%	0.075
900°C	85%	1.440
950°C	85%	2.550
1000°C	80%	2.488
1050°C	80%	1.538
1100°C	75%	1.399
1150°C	70%	1.134

from the rest of the simulations because of the amount of CO_2 in the recycle. Two basic trends were identified: the one trend was for the cases of T = 800°C and T = 850°C. The other trend was for the rest of the cases (T = 900°C – 1150°C). These trends can be seen in figure 5.3 and figure 5.4. To make the graphs more clear, the comparison of T = 800°C and T = 950°C were plotted together on figure 5.3 and the comparison of T = 950°C and T = 1150°C were plotted together on figure 5.4.

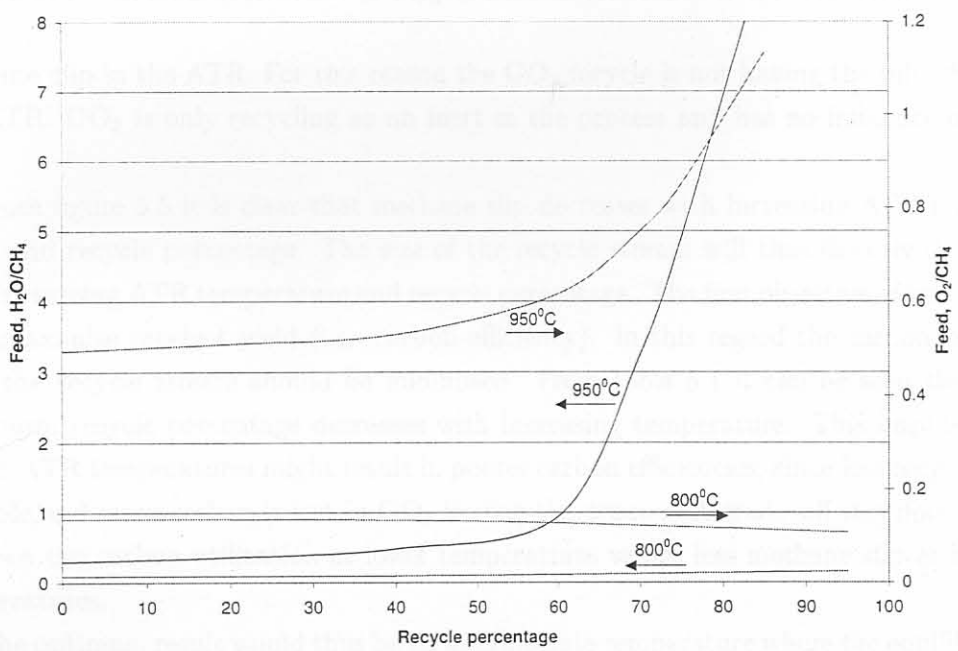

Figure 5.3: The steam/methane and oxygen/methane feed ratios to the ATR (1st scenario)

The trend for the T = 800°C case is due to the low temperature which encourages

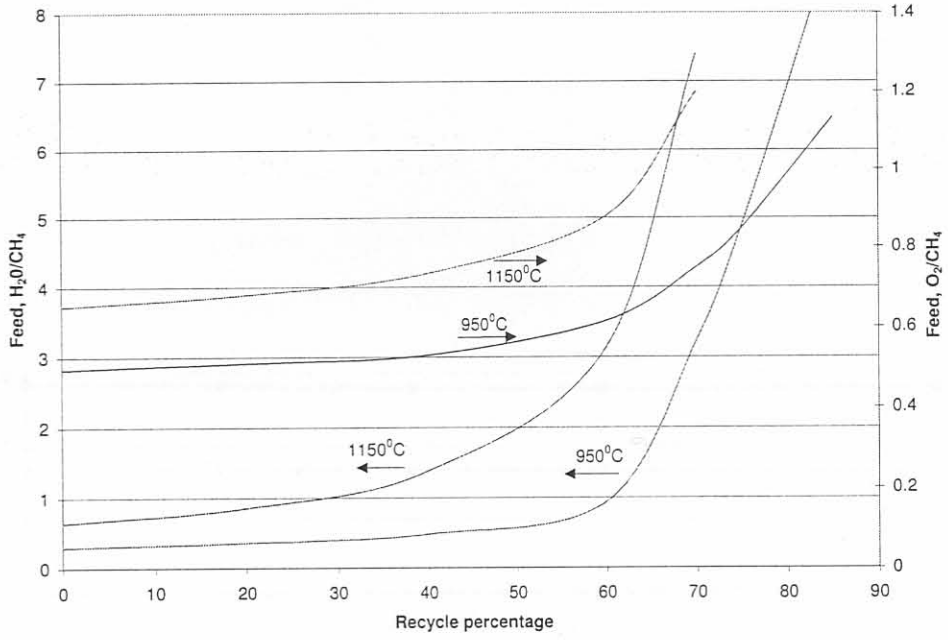

Figure 5.4: The steam/methane and oxygen/methane feed ratios to the ATR (2nd scenario)

methane slip in the ATR. For this reason the CO_2 recycle is not having the full effect in the ATR. CO_2 is only recycling as an inert in the process and has no influence on the ATR.

From figure 5.5 it is clear that methane slip decreases with increasing ATR temperature and recycle percentage. The size of the recycle stream will thus directly decrease with increasing ATR temperature and recycle percentage. The first objective of this study is to maximise product yield (i.e. carbon efficiency). In this regard the carbon purged from the recycle stream should be minimised. From table 5.1 it can be seen that the maximum recycle percentage decreases with increasing temperature. This implies that higher ATR temperatures might result in poorer carbon efficiencies, since less recycling is possible and more carbon is lost in CO_2 leaving the process. A trade–off therefore exists between the carbon utilization at lower temperatures versus less methane slip at higher temperatures.

The optimum result would thus be an intermediate temperature where the equilibrium in the reactor is sufficient to decrease methane slip and increase the external recycle percentage (which will contribute to a higher carbon efficiency). An added benefit will be the smaller amount of O_2 needed to maintain the ATR temperature as well as a smaller

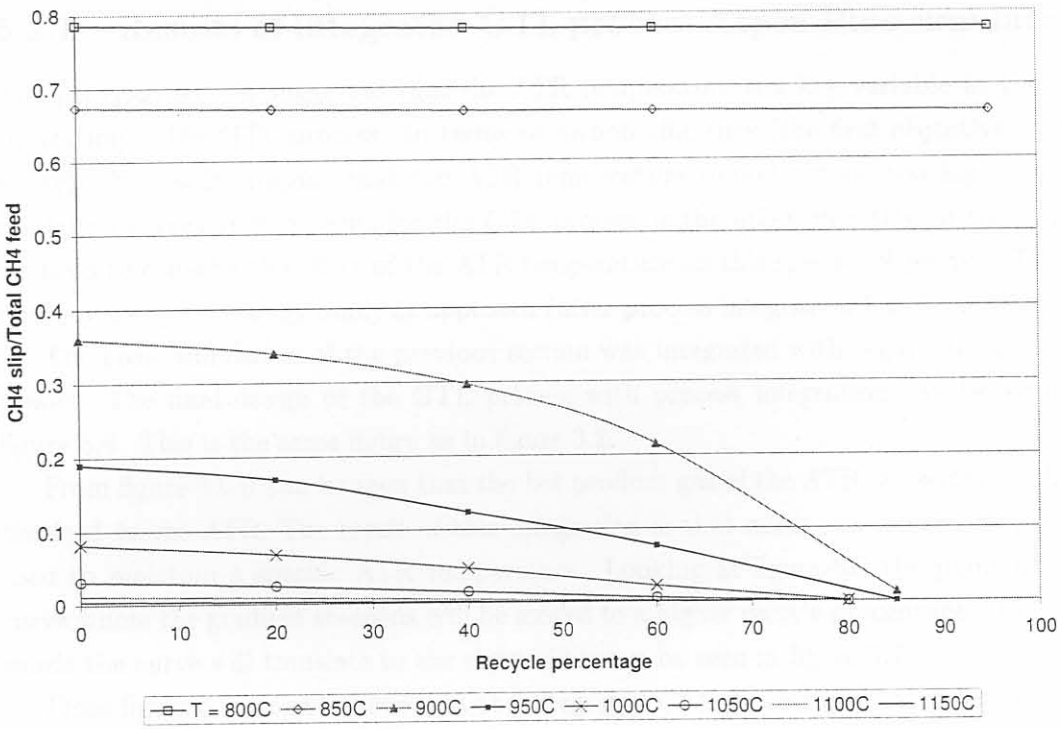

Figure 5.5: The methane slip percentage as a function of total methane fed to the ATR

H_2O/C ratio to maintain the desired H_2:CO ratio (see figures 5.3 and 5.4).

All of these simulations were done without any process integration. Integration will complicate the interaction between the units and could have a positive or negative influence on the process.

5.2 Determining optimum ATR temperature with exergy analysis and process integration

5.2.1 Results of integrated GTL process Aspen Plus simulation

The previous section suggested that the ATR temperature is a key variable in the optimization of the GTL process. In terms of carbon efficiency (the first objective of the study), the results suggest that the ATR temperature should not be too high. Since minimum energy requirements for the GTL process is the other objective of the study, we need to consider the effect of the ATR temperature on this specific objective. This is done by using the exergy analysis approach (after process integration has been done).

The basic simulation of the previous section was integrated with regard to heat and power. The final design of the GTL process with process integration can be seen in figure 5.6. This is the same figure as in figure 3.2.

From figure 5.6 it can be seen that the hot product gas of the ATR is used to preheat the feed to the ATR. The result of this integration is that much less oxygen has to be used to maintain a specific ATR temperature. Looking at figure 5.3 the point on the curve where the gradient steepens will be moved to a higher recycle percentage – in other words the curve will translate to the right. This can be seen in figure 5.7.

From figure 5.7 it can be seen that the integrated GTL process uses much less oxygen in the reformer than the non–integrated GTL process. Both the simulations were done at an ATR temperature of 900°C and a H_2:CO syngas ratio of 2.15.

Results for maximum external recycling and optimum feed to ATR

An integrated Aspen Plus simulation of the GTL process was used for varying the ATR temperature with maximum CO_2 recycling to the reformer. The H_2:CO syngas ratio was again kept at 2.15 with the minimum H_2O/C and O_2/C feed ratio. Temperatures of the ATR were varied between 905°C and 1170°C. The maximum recycle percentages that were achieved while maintaining a H_2:CO syngas ratio of 2.15 can be seen in table

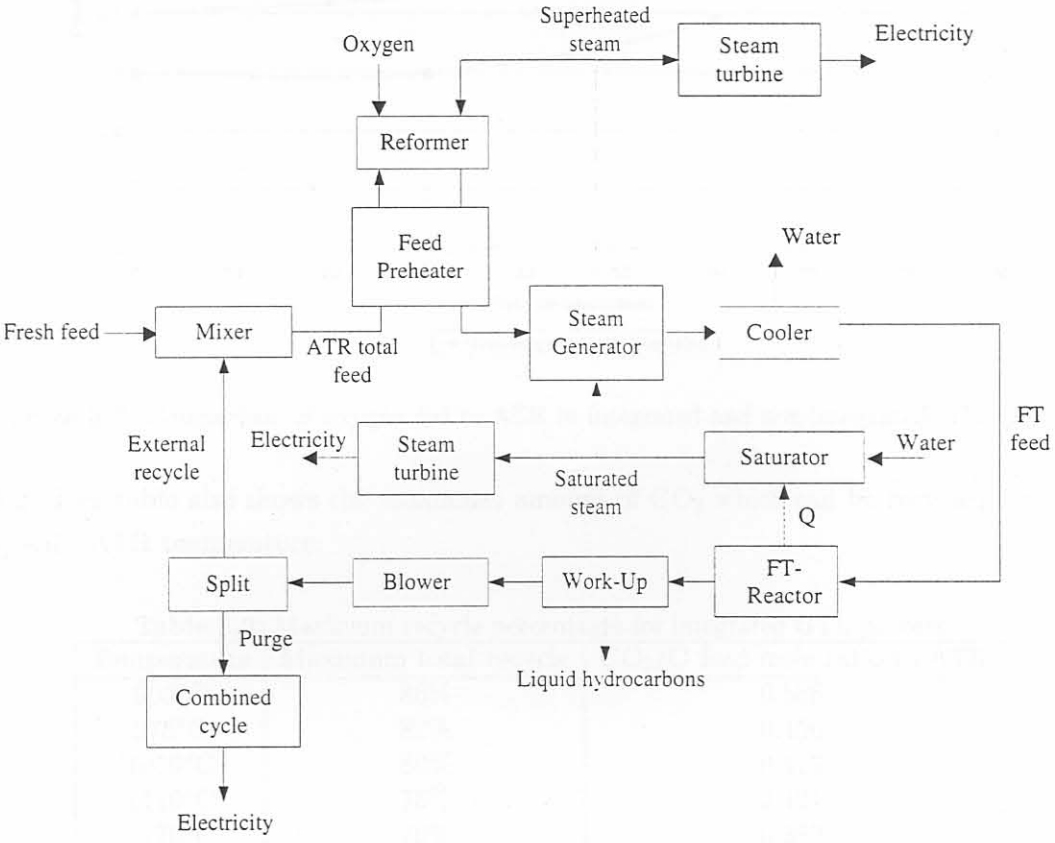

Figure 5.6: The final design of the GTL process with process integration

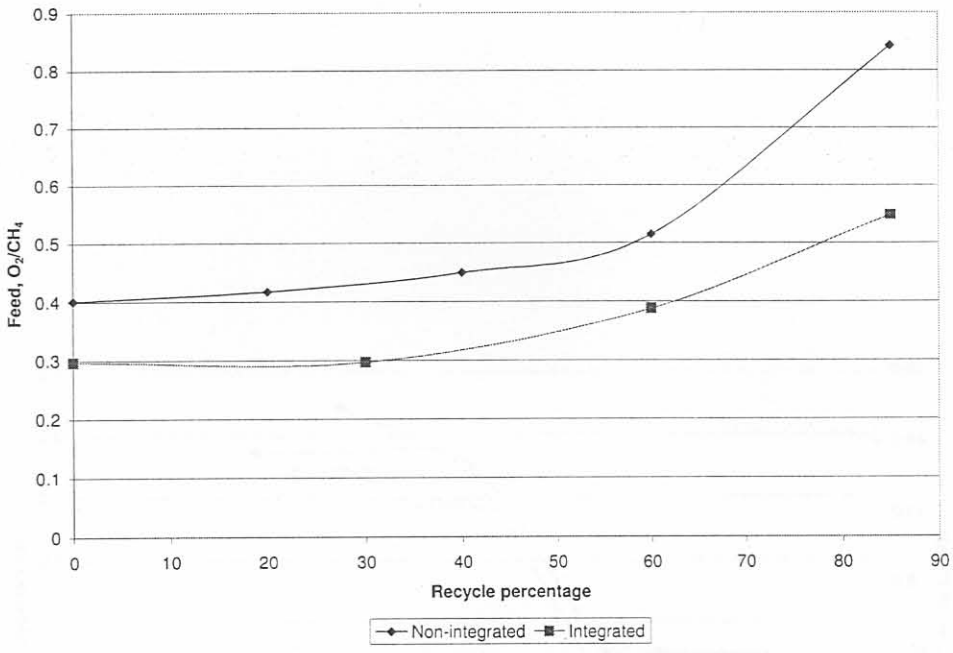

Figure 5.7: Comparison of oxygen fed to ATR in integrated and non-integrated GTL process

5.2. This table also shows the maximum amount of CO_2 which can be recycled for this specific ATR temperature.

Table 5.2: Maximum recycle percentages for integrated GTL process

Temperature	Maximum total recycle	CO_2/C feed mole ratio to ATR
905°C	86%	0.566
975°C	82%	0.456
1010°C	80%	0.413
1110°C	75%	0.421
1170°C	70%	0.362

The result of the simulation for the feed to the ATR can be seen in figure 5.8.

The steam/carbon feed ratio in figure 5.8 shows that the minimum feed results between 905°C and 1010°C. But with regard to expensive oxygen use, the lowest temperature possible would be the optimum.

Table 5.2 clearly indicates that a lower temperature in the ATR would result in higher maximum external recycling which would imply higher carbon efficiencies. The carbon efficiencies can be seen in figure 5.9.

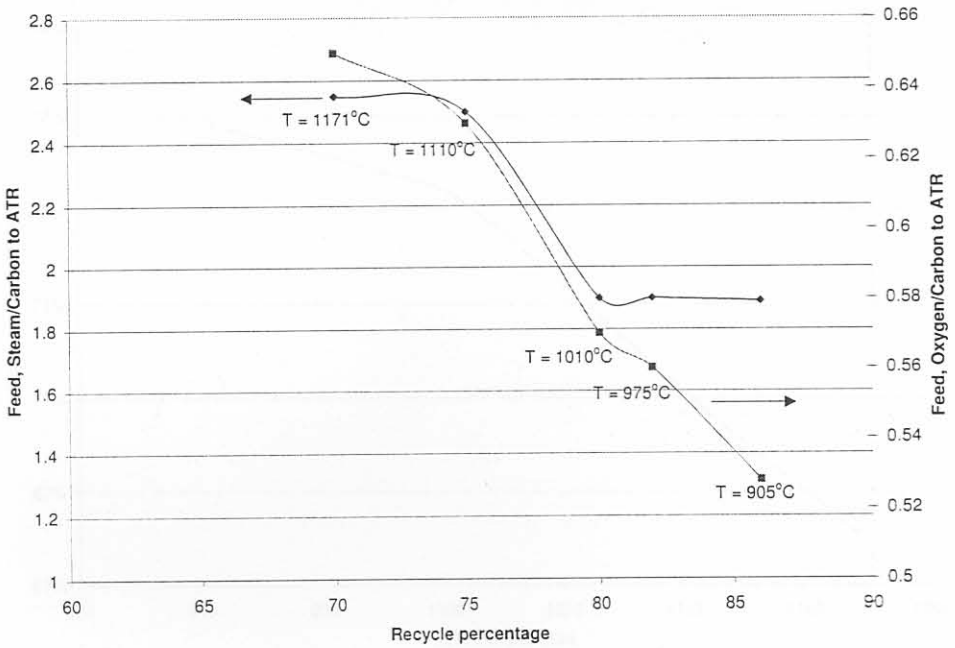

Figure 5.8: The steam/carbon and oxygen/carbon feed ratio to the ATR at maximum recycle (integrated process)

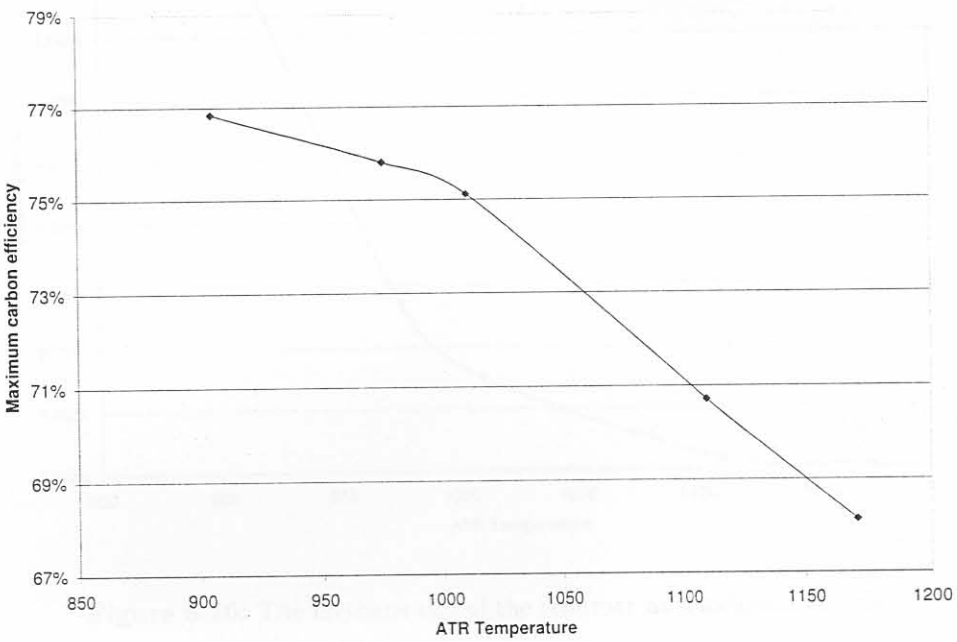

Figure 5.9: The maximum carbon efficiencies of the GTL process at different ATR temperatures

It can be seen from figure 5.9 that the carbon efficiency of the GTL process decreases with an increase in ATR temperature (extreme values between 77% for ATR T = 905°C and 68% for ATR T = 1171°C). Therefore the carbon efficiency would also be maximised with the lowest possible ATR temperature. The only negative impact of the high rate of external recycling is the increase in methane slip in the reformer. The results of the methane slip can be seen in figure 5.10.

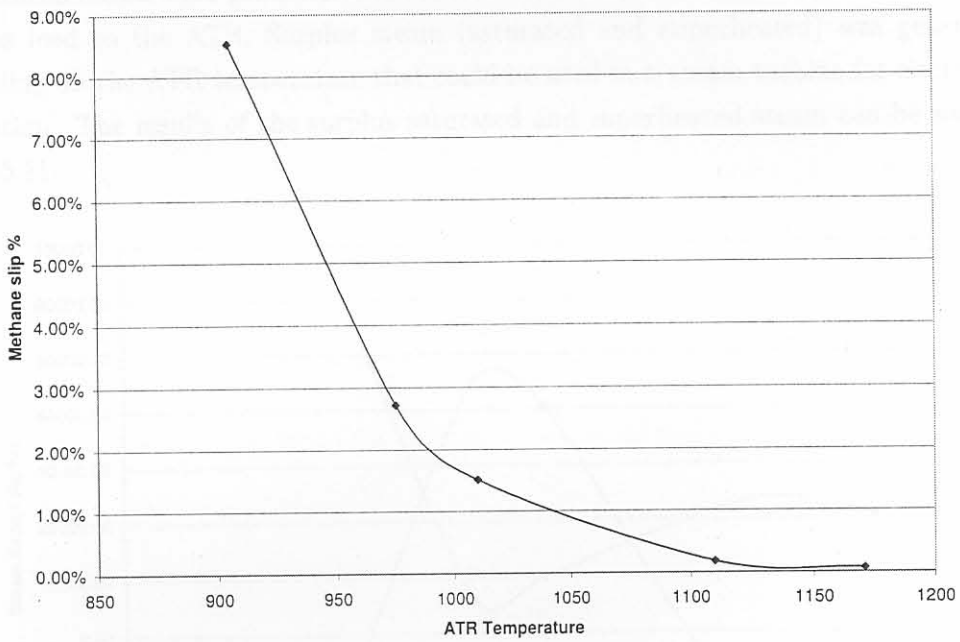

Figure 5.10: The methane slip of the reformer at maximum recycle

From the results of the methane slip in the reformer it is clear that the methane slip decreases with an increase in ATR temperature. This implies that we would rather want to operate the ATR at a higher temperature, because CH_4 conversion increases with a decrease in methane slip. But a methane slip of 8.53% (the highest case in this study) is still acceptable. From Rostrup-Nielsen (2002) it is known that acceptable CH_4 conversions of 70% can be attained with a methane slip of 8%. Thus for this study the lowest operating ATR temperature of 905°C has an acceptable methane slip.

Results for steam and electricity generation

The heat and power integration also provides a new design variable which should be considered – electricity generation. But before the results of the electricity generation can

be analysed, the amount of steam exported for electricity generation should be considered. Since all steam was generated at a pressure of 24 bar, the steam was divided into saturated (222°C) and superheated (430°C) steam. The saturated steam was generated with the heat from the Fischer–Tropsch reactor and the superheated steam with the heat from the reformer product gas. The saturated steam generated with the FT reactor was used as feed to the superheated steam generation. The maximum amount of saturated and superheated steam were generated with the heat available. The superheated steam was used as feed to the ATR. Surplus steam (saturated and superheated) was generated depending on the ATR temperature that could be used in a steam turbine for electricity generation. The results of the surplus saturated and superheated steam can be seen in figure 5.11.

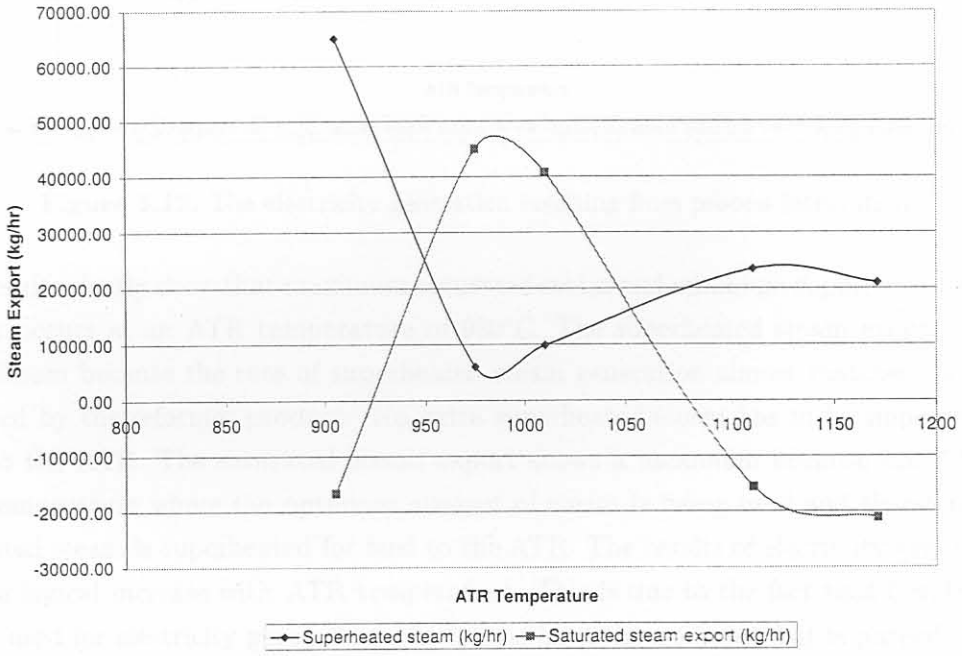

Figure 5.11: The surplus steam for electricity generation resulting from process integration

These results will be discussed together with the results of electricity generation which can be seen in figure 5.12.

Firstly it should be mentioned that the negative values on the surplus steam figure indicate that extra saturated steam had to be generated (or could be imported). This implies that import heat was necessary to generate sufficient saturated steam for feed to the superheated steam generator, because the heat from the FT reactor was not enough.

5.2.2 Results of the exergy analysis

Exergy losses and target exergy values for different ATR temperature scenarios

The exergy results can be seen in figures 5.13 and 5.14.

Table 5.3 presents energy and exergy figures for the different ATR temperatures on an absolute basis per unit C_5–C_{25} yield. Since absolute exergy losses are invariant and directly reflect the amount of work–potential being lost, regardless of the total amount of incoming energy and exergy, these are recommended rather than exergetic efficiencies when reporting on exergy analysis.

According to Hinderink *et al.* (1996) exergetic efficiencies are a more ambiguous measure, since they can be defined in numerous ways.

From table 5.3 it is clear that the amount of natural gas needed to make one ton of product increases with an increase in ATR temperature. With the exception of the process inputs water and air, which do not significantly contribute to the overall incoming energy and exergy, all inputs are associated with the application of natural gas, when generation efficiencies for power and import exergy are accounted for.

Approximately, 56–62% of the total incoming exergy is retained in the C_5–C_{25} product. This is known as target exergy and is also shown in figure 5.14. The exergy loss figures in the table are also represented in figure 5.13. These results will now be discussed along with figures 5.13 and 5.14.

The total exergy losses can be divided into internal and external exergy losses. Internal losses, also called irreversibilities, take place due to internal degradation of energy, while external losses can occur if process streams are emitted into the environment. From the results it can be seen that the total exergy loss increases with an increase in ATR temperature. The loss is at an even steeper gradient when the temperature is above 1010°C. This clearly indicates that the GTL process should rather be run at a low ATR temperature. This result is also supported by the results of the exergy contained in the product and is even more specific at which temperature the ATR should be run. If the exergy contained in the product is divided by the total exergy input, a maximum is obtained at an ATR temperature of 975°C. The actual exergy contained in the product decreases with an increase in ATR temperature and this is due to the lower carbon efficiency with higher ATR temperature. This result is based upon target exergy. Target exergy is denoted as a comparison between the actual input of exergy to exergy stored in the final product. In theory, a quantity of exergy equal to the target exergy, more or less

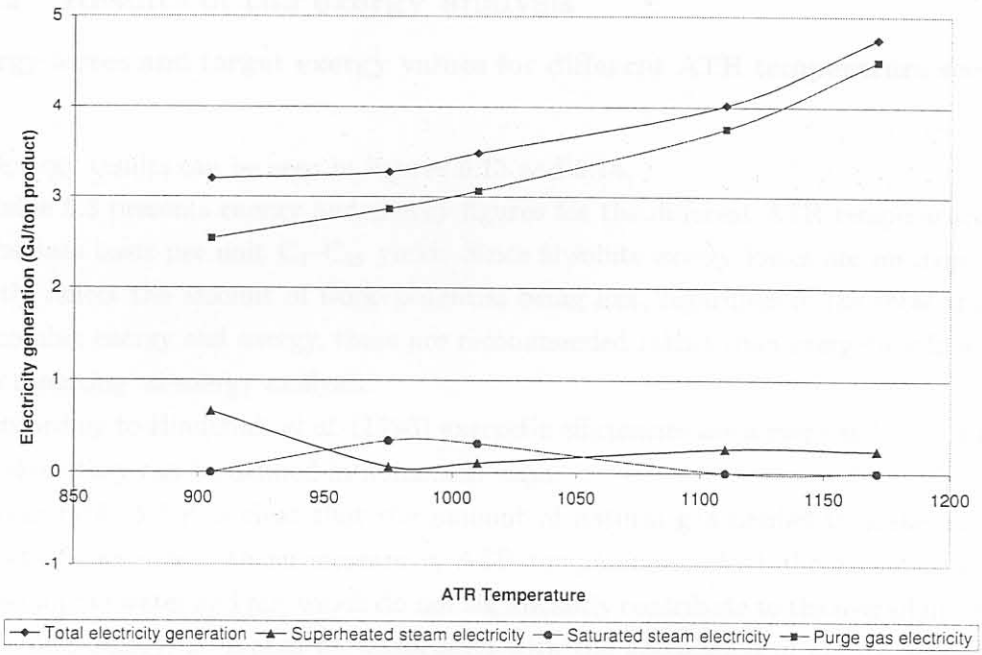

Figure 5.12: The electricity generation resulting from process integration

The results clearly show that maximum saturated steam and minimum superheated steam export occurs at an ATR temperature of 980°C. The superheated steam export shows a minimum because the rate of superheated steam generation almost matches the heat supplied by the reformer product. No extra superheated steam has to be imported for feed to the ATR. The saturated steam export shows a maximum because the ATR is at a temperature where the optimum amount of steam is being used and therefore less saturated steam is superheated for feed to the ATR. The results of electricity generation show a logical increase with ATR temperature. This is due to the fact that besides the steam used for electricity generation, the tailgas from the work-up that is purged at the recycle split is also used for electricity generation. From the previous results discussion it is known that the amount of purge gas increases with an increase in ATR temperature. Thus more electricity will be generated at higher ATR temperatures, also due to the fact that more heat is available. *It should be kept in mind that the goal of the process is to make a diesel product and not to generate electricity.*

With this steam and electricity generation in mind the discussion could now be focused on the exergy analysis results.

Table 5.3: Energy and exergy figures for various ATR temperatures

					Useful exergy output (GJ/t product)		Exergy loss (GJ/t product)		
T	Feedstock NG (N m^3/t product)	Fuel NG (N m^3/t product)	Total energy input (GJ/t product)	Total exergy input (GJ/t product)	C_5–C_{25} product	Electricity	Internal	External	Total
905°C	2075	145	58.0	77.5	48.7	3.2	18.43	6.73	25.15
975°C	2103	154	56.9	77.2	48.7	3.3	18.70	7.36	26.07
1010°C	2122	162	57.4	77.8	48.7	3.5	18.98	7.77	26.76
1110°C	2254	258	57.1	83.3	48.7	4.0	23.37	9.42	32.79
1170°C	2340	298	58.9	86.8	48.7	4.7	25.43	11.01	36.44

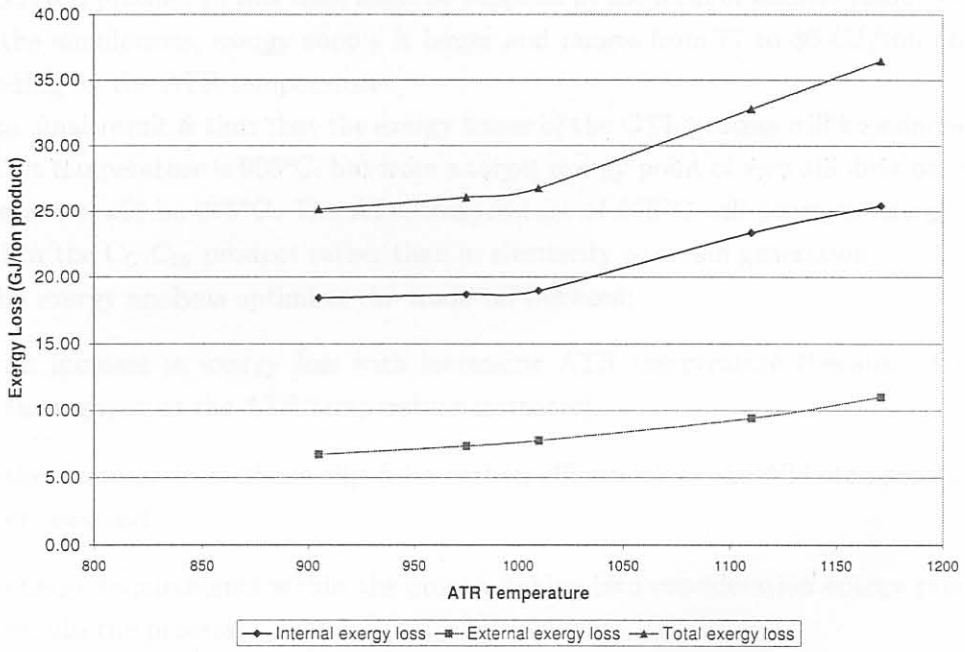

Figure 5.13: The total exergy loss (internal and external) of the GTL process

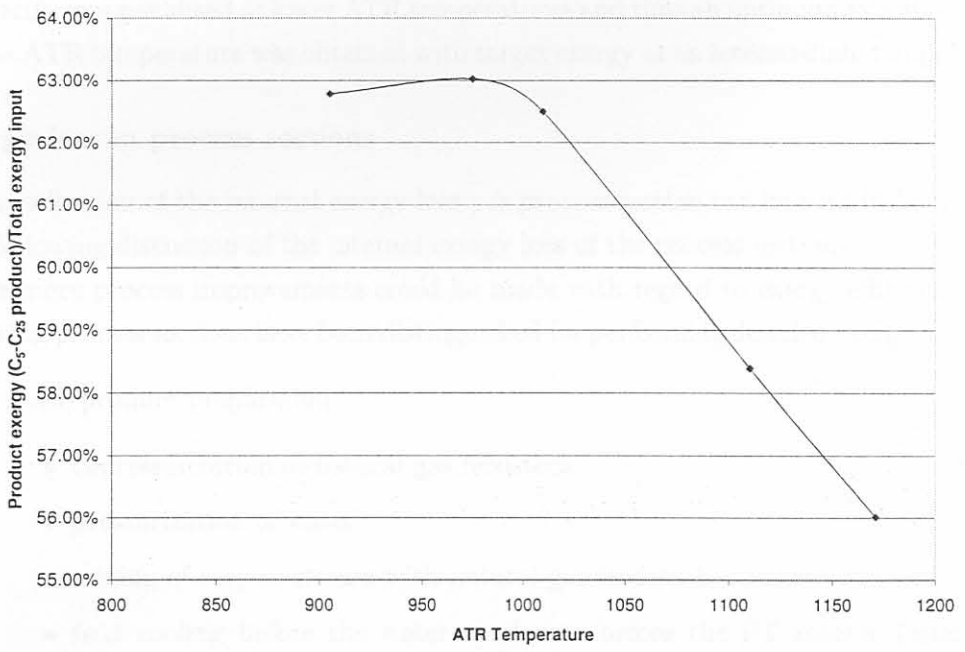

Figure 5.14: The exergy contained in the C_5 – C_{25} product of the GTL process

48.7 GJ/ton product in this case, must be supplied in the form of natural resources. But from the simulations, exergy supply is larger and ranges from 77 to 86 GJ/ton product depending on the ATR temperature.

The final result is thus that the exergy losses of the GTL process will be minimised if the ATR temperature is 905°C, but from a target exergy point of view the best operating temperature will be 975°C. The ATR temperature of 975°C will promote exergy to be stored in the C_5–C_{25} product rather than in electricity or steam generation.

The exergy analysis optimises the trade–off between:

- an increase in exergy loss with increasing ATR temperature (because of bigger throughput as the ATR temperature increases),
- the decrease in methane slip (also carbon efficiency) as the ATR temperature increases and
- energy requirements within the process taking into consideration energy produced within the process.

An advantage of exergy analysis is that all products of the process (including export electricity) can be evaluated and compared. Misdirected energy in the form of export electricity was penalised at lower ATR temperatures and thus an optimum exergy solution for the ATR temperature was obtained with target exergy at an intermediate temperature.

Exergy loss in process sections

The subdivision of the internal exergy loss per process section can be seen in figure 5.15. The following discussion of the internal exergy loss of the process sections could indicate where more process improvements could be made with regard to exergy efficiency. The following process sections have been distinguished for performing detailed exergy analyses:

1. Feed/product preparation
    - depressurization of natural gas feedstock
    - pressurization of water
    - mixing of recycle stream with natural gas feedstock
    - feed cooling before the water condenser before the FT reactor (after heat exchange with ATR feed and superheated steam generation)
    - feed preheating to the FT reactor

- blower in recycle to the ATR.

2. ATR reaction section
   - autothermal reformer
   - mixing feeds
3. Heat recovery – ATR reaction section
   - feed preheater
   - steam generator
4. SBR reaction section
   - SBR reactions
5. Heat recovery – SBR reaction section
   - saturated steam generation with heat from SBR
6. Air separation
   - air compressors
   - oxygen and nitrogen separation
7. Power generation
   - generation of electricity with saturated and superheated steam
   - generation of electricity with combined cycle (purge tailgas)

As could be seen from figure 5.13, the overall internal exergy loss increases with an increase in ATR temperature. Figure 5.15 shows a more detailed subdivision of the reasons for the increase in exergy loss.

The feed/product preparation internal exergy loss increase tremendously with an increase in ATR temperature, mainly because of the large amount of cooling that has to be done for the water to condense during feed preparation before the SBR.

The exergy losses in the ATR reaction section also increase with an increase in temperature, because the thermodynamic driving forces become too large and are unnecessary.

The heat recovery section for the ATR shows lowest internal exergy losses at a temperature of 1010°C. This is due to the large amount of saturated steam available for

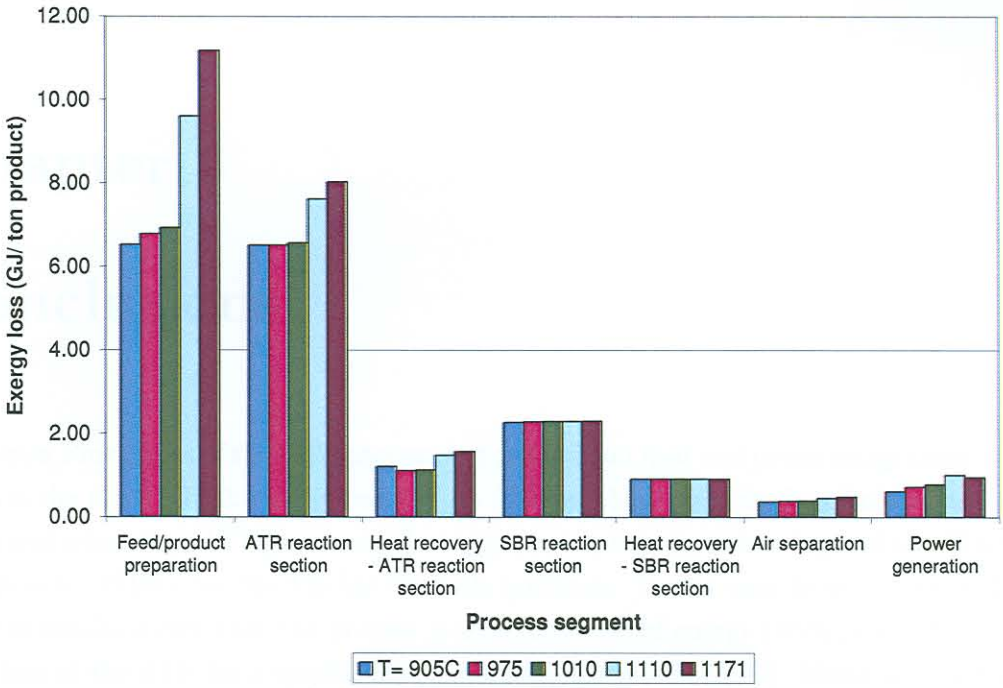

Figure 5.15: Subdivision of internal exergy loss per process section

superheated steam generation and also because of a very good ΔT for the feed preheat exchanger (best ΔT in all simulations).

The conditions in the SBR didn't change with the change in the ATR temperature and thus the internal exergy loss for all the simulations remained constant. The same with the heat recovery for the SBR reaction section.

The contribution of the air separation internal exergy losses are small compared to the other process sections. The exergy losses do increase with a need for more oxygen as the ATR temperature increases.

The losses with the power generation also increases as the internal exergy loss with the larger purge gas combustion increase.

The final remark is that the largest contributors to internal exergy loss are the feed/product preparation and the ATR reaction section. Further improvements in a follow-up study in these sections could result in ultimate optimization.

Chapter 6

Conclusions

An Aspen Plus model of the GTL process was created and heat and power integration was done on the model. High quality natural gas (95% methane) was used as feedstock. Autothermal reforming (ATR) was considered the best option for reforming and the Slurry Bed Reactor (SBR) for the Fischer–Tropsch synthesis. It was seen from a total GTL reaction stoichiometry that the process is a net exporter of energy (with near adiabatic operation of the ATR for a specific Schulz–Flory alpha value of 0.95). Maximum carbon efficiency could also be obtained without separating CO_2 directly after the reformer, but rather recycling the tailgas externally from the work–up to the reformer. This tailgas consists mostly of CO_2.

The heat integration was focused on recovering heat from the Fischer-Tropsch reactor, from the reformer and from the purge stream (necessitated by the external recycle - see figure 5.6). Maximum carbon ATR feed preheating was done within a heat exchanger between the carbon feed and the ATR product stream. It was assumed that no sooting would occur and that such a heat exchanger was possible for estimating optimum heat recovery from the ATR (thus idealistic). Steam used as feed to the ATR was generated with excess ATR product heat and saturated steam was generated with SBR reaction heat. Any surplus steam generated was used in a steam turbine to generate electricity to be used in the GTL process. The work–up tailgas that was not recycled to the ATR, was combusted in a combined cycle process to generate electricity for use in the process. The amount of steam generated and thus electricity generated depends on the ATR temperature.

The effect of different ATR temperatures were investigated with the following constraints:

- The H_2:CO syngas ratio (product of ATR) was kept constant at 2.15 to maintain

a Schulz–Flory alpha value of 0.95 in the SBR.

- The maximum amount of work–up tailgas was externally recycled to the reformer while maintaining the H_2:CO syngas ratio at 2.15.
- Minimum steam and oxygen feeds were used in the ATR to maintain the H_2:CO ratio of 2.15 and the specified ATR temperature.

It was shown in this work that lower ATR temperatures compared to typical commercial ATR temperatures can increase the carbon efficiency of an integrated GTL process without significantly increasing the methane slip (taking the assumptions into consideration). The reason for this being that more tailgas recycling is possible at lower temperatures, i.e. more CO_2 can be processed in the reformer while maintaining the desired H_2:CO ratio in the reformer product. While the lower ATR temperature results in an increase in methane slip, the CO_2 recycle helps to reduce the methane slip up to a point where the H_2:CO syngas ratio cannot be maintained. The lower ATR temperature also implicates that lower O_2/C and H_2O/C feed ratios to the ATR are required.

Target exergy analysis was used as an optimization tool for finding the optimum ATR temperature of 975°C. This optimum ATR temperature considers the trade–off between methane slip, carbon efficiency and energy utilization. At the optimum ATR temperature of 975°C the methane slip is 2.7% (still within an acceptable range), the improvement in carbon efficiency is 7% compared to the carbon efficiency at 1100°C and the total exergy loss is 26% lower than the total exergy loss at 1100°C. At the optimum temperature the energy is utilized in such a manner that the maximum exergy is stored in the final product (i.e. liquid hydrocarbons) and not in utilities (i.e. electricity) produced by the process.

The integrated GTL layout in this study was just the first iteration in a process of finding the optimum integrated GTL layout. The exergy analysis showed that the largest contributors to internal exergy loss are the feed/product preparation sections and the ATR reaction section. Further improvements in a follow–up study of these sections could result in further optimization. The exergy analysis will also assist a cost benefit analysis in a follow–up study to motivate the integration investment costs.

Chapter 7

Recommendations

The recommendations that result from this study:

- Incorporate selectivity into Fischer–Tropsch reactor model to implement trade–off between between a decrease in selectivity and an increase in reaction rate for a higher H_2:CO ratio in the syngas.
- Improve feed/product preparation process sections and also the ATR reaction section to decrease internal exergy losses.
- Use pinch analysis together with exergy analysis to optimise use of heat in GTL process.
- Do a cost analysis for trade–off between profits gained in energy savings and product yield vs. investment costs for start–up equipment.
- Design procedures for process synthesis, exergy and pinch analysis integration.
- Compare the results of the exergy analysis to the results of a cost analysis.

Bibliography

Christensen, T. and Primdahl, I. (1994) "Improve syngas production using autothermal reforming", *Hydrocarbon Processing, 3*, 39–46.

Ernst, W.; Venables, S.; Christensen, P. and Berthelsen, A. (2000) "Push syngas production limits", *Hydrocarbon Processing, 29* (3), 100C–100J.

Espinoza, R. L.; Steynberg, A. P.; Jager, B. and Vosloo, A. C. (1999) "Low temperature Fischer-Tropsch synthesis from a Sasol perspective", *Applied Catalysis A: General, 186*, 13–26.

Futterer, E.; Gruhn, G.; Lohe, B.; Noronha, S. and Rucker, A. (1996) "Exergy as an objective function to MINLP problems in process synthesis", *Chemical Engineering technology, 19*, 203–208.

Hill, C. (1998) "What makes a natural gas to liquid fuels project viable?", *Middle East Petroleum and Gas Conference, Sasol Synfuels International*, 1–6.

Hinderink, A.; Kerkhof, F.; Lie, A.; de Swaan Arons, J. and van der Koof, H. (1996) "Exergy analysis with a flowsheeting simulator - ii. Application: Synthesis gas production from natural gas", *Chemical Engineering Science, 51* (20), 4701–4715.

Jager, B. (1998) "Developments in Fischer-Tropsch technology", *Natural Gas Conversion V, 119*, 25–34.

Jager, B. and Espinoza, R. (1995) "Advances in low temperature Fischer-Tropsch synthesis", *Catalysis Today, 23*, 17–28.

Karp, A.; Korens, N.; Simbeck, D.; Biasca, F.; Dickenson, R. and Johnson, H. (1998) *Hydrogen and Synthesis Gas: Technology, Economics, and Market Outlook, a private multiclient-sponsored analysis*, SFA Pacific, California, United States.

Kerkhof, F. and van Steenderen, P. (2000) *Integration of gas turbine and air separation unit for IGCC power plants: study on efficiency of IGCC under aspect of exergy*, Netherlands agency for Energy and Environment (NOVEM), Eindhoven, The Netherlands.

Kölbel, H. and Ralek, M. (1980) "The Fischer-Tropsch synthesis in the liquid phase", *Catalyst Reviews - Science and Engineering, 21* (2), 225–274.

Kotas, T. (1985) *The Exergy Method of Thermal Plant Analysis*, Butterworths, Department of Mechanical Engineering, Queen Mary College, University of London.

Loonen, T.; Prins, M.; Ptasinski, K. and Janssen, F. (2001) *Exergie-analyse van de productie van Fischer-Tropsch vloeistoffen door vergassing van biomassa*, Chemical Reactor Technology, Technical University of Eindhoven, Eindhoven, The Netherlands.

Lox, E. S. and Froment, G. F. (1993) "Kinetics of the Fischer-Tropsch reaction on a precipitated promoted iron catalyst 2", *Ind. Eng. Chem. Res, Kinetic Modelling* (32), 71–82.

Lutz, B. (2001) "New age gas-to-liquids processing", *Hydrocarbon Engineering, November*, 23–27.

Rostrup-Nielsen, J. (2002) "Syngas in perspective", *Catalysis Today, 71*, 243–247.

Smith, J.; van Ness, H. and Abbott, M. (1996) *Introduction to Chemical Engineering Thermodynamics*, Chemical Engineering Series McGraw-Hill International, fifth edition.

Szargut, J.; Morris, D. and Steward, F. (1988) *Exergy analysis of thermal, chemical, and metallurgical processes*, Springer-Verlag, Berlin.

Union-Gas (May 2002) *Natural Gas Composition*, About Natural Gas, www.uniongas.com.

van Schijndel, P.; Ptasinski, K. and Janssen, F. (2001) *Evaluation of Tools for a Cleaner Chemical Industry*, Efficiency, Cost, Optimization, Simulation and Environmental Impact of Energy Systems First International Conference on Applied Thermodynamics, Istanbul.

Vosloo, A. (2001) "Fischer-Tropsch: a futuristic view", *Fuel Processing Technology, 71*, 149–155.

Wilhelm, D.; Simbeck, D.; Karp, A. and Dickenson, R. (2001) "Syngas production for gas-to-liquids applications:technologies, issues and outlook", *Fuel Processing Technology, 71*, 139–148.

Williams, R. and Larson, E. (1993) *Advanced gasification-based biomass power generation*, Renewable energy: sources for fuels and electricity, Island Press, Washington D.C.

Appendix A

Process synthesis

When analyzing the GTL process and the overall stoichiometry of the process it can be shown that the process is a net exporter of energy (see equation A.5). This was already shown in the main part of the report, but is given again in this section to show the importance of this fact.

If we are interested in what H_2:CO syngas ratio we can ideally obtain without having any CO_2 we can do the following: Take one mol of methane and reform 0.8 mol and burn 0.2 mol (for ideal adiabatic combustion). Take the 0.2 mol of CO_2 and shift it by using 0.2 mol of H_2 from the reforming section. The result is 0.8 + 0.2 = 1 mol of CO, 2.4 - 0.2 = 2.2 mol of H_2, which gives a H_2:CO ratio of 2.2:1 for a 100% C efficiency. Comparing this ratio to the ratio of 2.15 used in this study, there is not much of a difference. This H_2:CO ratio of 2.15 was necessitated by the fact that we want a Schulz–Flory alpha value of 0.95 in the SBR (refer once again to the main report). See equations A.1, A.2, A.3 for the reactions taking place in the reformer and equation A.4 for the reaction taking place in the SBR.

$$0.7875CH_4 + 0.7878H_2O \rightleftharpoons 0.7875CO + 2.3625H_2 \qquad \Delta_r H^0 = +162.5\frac{kJ}{mol} \quad \text{(A.1)}$$

$$0.2125CH_4 + 0.425O_2 \rightarrow 0.2125CO_2 + 0.425H_2O \qquad \Delta_r H^0 = -170.5\frac{kJ}{mol} \quad \text{(A.2)}$$

$$0.2125CO_2 + 0.2125H_2 \rightleftharpoons 0.2125CO + 0.2125H_2O \qquad \Delta_r H^0 = +8.6\frac{kJ}{mol} \quad \text{(A.3)}$$

$$CO + 2.15H_2 \rightarrow -CH_2 - +H_2O + 0.15H_2 \qquad \Delta_r H^0 = -203\frac{kJ}{mol} \quad \text{(A.4)}$$

When combining all of the above equations, the resulting equation can be seen in equation

A.5.

$$CH_4 + 0.425O_2 \rightarrow -CH_2 - +0.85H_20 + 0.15H_2 \qquad \Delta_r H^0 = -202.4\frac{kJ}{mol} \tag{A.5}$$

Thus from equation A.5 it can be seen that a surplus of 0.15 mol of H_2 will be produced for every 1 mol of CH_4 fed to the reformer. This is for near ideal adiabatic conditions in the ATR. This equation also shows that the process will be a net exporter of energy. The idea was thus to design the process to realise this goal. But it was kept in mind that the export of energy would only be possible with a very high total carbon efficiency (which is not always practical). This led to the main objectives for designing this process:

- optimization of product yield (i.e. maximum carbon efficiency) and
- minimum energy requirements.

Appendix B

The SBR product distribution

The importance of the H_2:CO consumption ratio in the Fischer-Tropsch reactor was already discussed in the literature survey. This ratio will determine the product distribution in the Fischer-Tropsch reactor, together with the type of catalyst, temperature and reactor type. To manipulate the H_2:CO ratio of the syngas in the ATR, either the temperature, S/C ratio, O_2/C ratio or the amount of CO_2 recycled can be used (Ernst *et al.*, 2000).

In this study the specific syngas H_2:CO consumption ratio is 2.15 to obtain a Schulz-Flory alpha value of 0.95. Refer here to figure B.1 and to the literature survey on H_2:CO ratios and the Schulz-Flory alpha values. The H_2:CO consumption ratios were calculated by determining the product distribution according to the Flory–Schulz distribution (see equation B.1)

$$y_n = (1-p)p^{(n-1)} \tag{B.1}$$

and then determining the H_2:CO consumption ratios accordingly (see equation B.2):

$$ratio = \frac{2n+1}{n} \cdot y_n \tag{B.2}$$

It is also known that a higher H_2:CO ratio would increase the reaction rate, but can decrease the selectivity. For this study it was assumed that a syngas H_2:CO ratio of 2.15 is sufficient for a reasonable selectivity and a high rate of reaction.

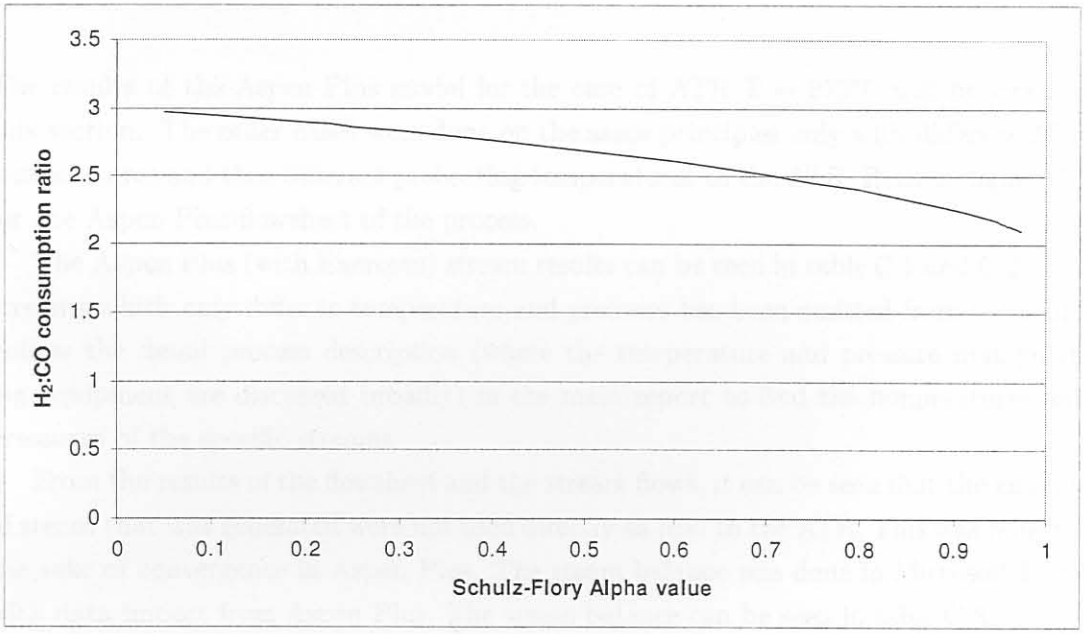

Figure B.1: The H_2:CO consumption ratios

Appendix C

Aspen Plus modelling results

The results of the Aspen Plus model for the case of ATR T = 975°C will be given in this section. The other cases were done on the same principles only with different ATR temperatures and thus different preheating temperatures to the ATR. Refer to figure C.1 for the Aspen Plus flowsheet of the process.

The Aspen Plus (with Exercom) stream results can be seen in table C.1 and C.2. The streams which only differ in temperature and pressure has been omitted from the table. Follow the detail process description (where the temperature and pressure manipulating equipment are discussed broadly) in the main report to find the temperatures and pressures of the specific streams.

From the results of the flowsheet and the stream flows, it can be seen that the amount of steam that was generated were not used directly as feed to the ATR. This was done for the sake of convergence in Aspen Plus. The steam balance was done in Microsoft Excel with data import from Aspen Plus. The steam balance can be seen in table C.3.

As can be seen from table C.3 the steam generated on the plant was integrated between the Fischer-Tropsch reactor and the ATR. The Fischer-Tropsch reactor operates at 260°C and therefore it can only produce saturated steam at the required pressure. The maximum amount of saturated steam was produced in each scenario for the heat available from the FT reactor.

This saturated steam was then superheated by the hot exit gases from the ATR. The superheated steam generated was then used as feed to the ATR.

In both cases (the FT reactor and the ATR) if surplus steam were generated, the surplus steam was sent through a steam turbine to generate electricity. In some cases (very low and very high ATR temperatures) more saturated steam had to be imported for producing enough superheated steam as feed to the ATR.

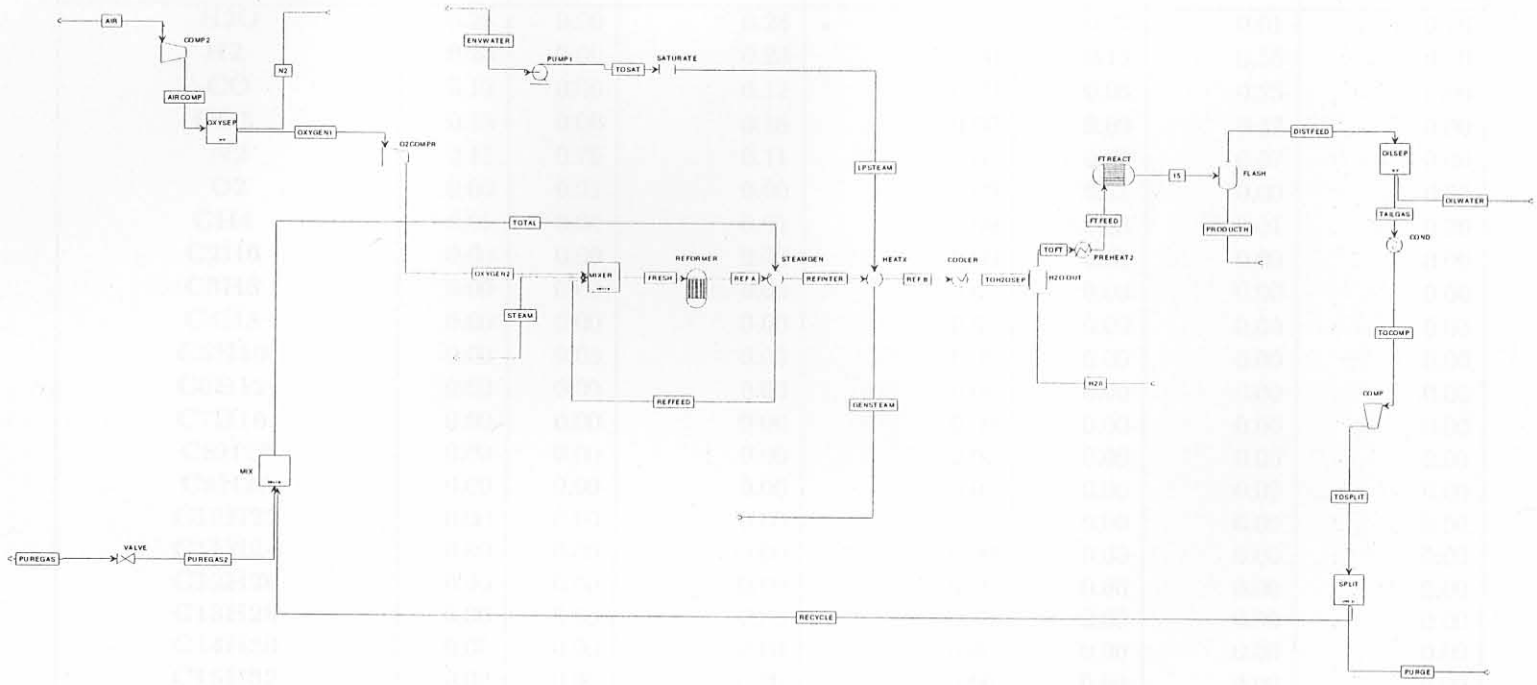

Figure C.1: The Aspen Plus process flowsheet for the GTL process

Table C.1: Stream results for the case of ATR T=975°C

Mole Fraction	15	AIR	DISTFEED	ENVWATER	FRESH	FTFEED	OILWATER
H2O	0.28	0.00	0.28	1.00	0.37	0.01	0.96
H2	0.28	0.00	0.28	0.00	0.13	0.55	0.00
CO	0.12	0.00	0.12	0.00	0.06	0.25	0.00
CO2	0.18	0.00	0.18	0.00	0.09	0.12	0.00
N2	0.11	0.79	0.11	0.00	0.06	0.07	0.00
O2	0.00	0.21	0.00	0.00	0.11	0.00	0.00
CH4	0.01	0.00	0.01	0.00	0.18	0.01	0.00
C2H6	0.00	0.00	0.00	0.00	0.01	0.00	0.00
C3H8	0.00	0.00	0.00	0.00	0.00	0.00	0.00
C4H8	0.00	0.00	0.00	0.00	0.00	0.00	0.00
C5H10	0.00	0.00	0.00	0.00	0.00	0.00	0.00
C6H12	0.00	0.00	0.00	0.00	0.00	0.00	0.00
C7H16	0.00	0.00	0.00	0.00	0.00	0.00	0.00
C8H18	0.00	0.00	0.00	0.00	0.00	0.00	0.00
C9H20	0.00	0.00	0.00	0.00	0.00	0.00	0.00
C10H22	0.00	0.00	0.00	0.00	0.00	0.00	0.00
C11H24	0.00	0.00	0.00	0.00	0.00	0.00	0.00
C12H26	0.00	0.00	0.00	0.00	0.00	0.00	0.00
C13H28	0.00	0.00	0.00	0.00	0.00	0.00	0.00
C14H30	0.00	0.00	0.00	0.00	0.00	0.00	0.00
C15H32	0.00	0.00	0.00	0.00	0.00	0.00	0.00
C16H34	0.00	0.00	0.00	0.00	0.00	0.00	0.00
C17H36	0.00	0.00	0.00	0.00	0.00	0.00	0.00
C18H38	0.00	0.00	0.00	0.00	0.00	0.00	0.00
C19H40	0.00	0.00	0.00	0.00	0.00	0.00	0.00
C20H42	0.00	0.00	0.00	0.00	0.00	0.00	0.00
C21H44	0.00	0.00	0.00	0.00	0.00	0.00	0.00
C22H46	0.00	0.00	0.00	0.00	0.00	0.00	0.00
C23H48	0.00	0.00	0.00	0.00	0.00	0.00	0.00
C24H50	0.01	0.00	0.00	0.00	0.00	0.00	0.01
Total Flow KMOL/HR	9764	8902	9713	6550	16891	15151	2884
Total Flow KG/HR	235522	256826	221473	118000	349172	235522	72504
Temperature C	260	25	261	25	716	260	261
Pressure BAR	23	1	23	1	24	23	23

Table C.2: Stream results (continued) for the case of ATR T=975°C

Mole Fraction	OXYGEN2	PRODUCTH	PUREGAS	RECYCLE	REF-A	REFFEED	STEAM
H2O	0.00	0.10	0.00	0.00	0.30	0.00	1.00
H2	0.00	0.01	0.00	0.40	0.39	0.26	0.00
CO	0.00	0.01	0.00	0.17	0.18	0.11	0.00
CO2	0.00	0.02	0.01	0.26	0.08	0.17	0.00
N2	0.07	0.01	0.02	0.15	0.05	0.11	0.00
O2	0.93	0.00	0.00	0.00	0.00	0.00	0.00
CH4	0.00	0.00	0.95	0.01	0.00	0.35	0.00
C2H6	0.00	0.00	0.03	0.00	0.00	0.01	0.00
C3H8	0.00	0.00	0.00	0.00	0.00	0.00	0.00
C4H8	0.00	0.00	0.00	0.00	0.00	0.00	0.00
C5H10	0.00	0.00	0.00	0.00	0.00	0.00	0.00
C6H12	0.00	0.00	0.00	0.00	0.00	0.00	0.00
C7H16	0.00	0.00	0.00	0.00	0.00	0.00	0.00
C8H18	0.00	0.00	0.00	0.00	0.00	0.00	0.00
C9H20	0.00	0.00	0.00	0.00	0.00	0.00	0.00
C10H22	0.00	0.00	0.00	0.00	0.00	0.00	0.00
C11H24	0.00	0.00	0.00	0.00	0.00	0.00	0.00
C12H26	0.00	0.00	0.00	0.00	0.00	0.00	0.00
C13H28	0.00	0.01	0.00	0.00	0.00	0.00	0.00
C14H30	0.00	0.01	0.00	0.00	0.00	0.00	0.00
C15H32	0.00	0.01	0.00	0.00	0.00	0.00	0.00
C16H34	0.00	0.01	0.00	0.00	0.00	0.00	0.00
C17H36	0.00	0.01	0.00	0.00	0.00	0.00	0.00
C18H38	0.00	0.02	0.00	0.00	0.00	0.00	0.00
C19H40	0.00	0.02	0.00	0.00	0.00	0.00	0.00
C20H42	0.00	0.03	0.00	0.00	0.00	0.00	0.00
C21H44	0.00	0.03	0.00	0.00	0.00	0.00	0.00
C22H46	0.00	0.03	0.00	0.00	0.00	0.00	0.00
C23H48	0.00	0.04	0.00	0.00	0.00	0.00	0.00
C24H50	0.00	0.62	0.00	0.00	0.00	0.00	0.00
Total Flow KMOL/HR	1973	51	3101	5599	21459	8701	6218
Total Flow KG/HR	62563	14049	52437	122155	349172	174591	112017
Temperature C	650	261	279	57	975	885	430
Pressure BAR	24	23	60	26	24	26	24

Table C.3: Steam balance for the case of ATR T=975°C

Type of steam	Value	Unit
Sat. steam generated by FT-Reactor	163006.1	kg/hr
Sat. steam used for superheated steam generation	118000.0	kg/hr
Sat. steam exported	45006.1	kg/hr
Sat. steam exported (Exergy)	11700558.4	Watt
Sat. steam exported (Exergy/ton product)	1.2	GJ / t C5-C25 product
Superheated steam generated	118000.0	kg/hr
Superheated steam exported	5990.0	kg/hr
Superheated steam exported (Exergy)	2099300.0	Watt
Superheated steam exported (Exergy/ton product)	0.2	GJ / t C5-C25 product

The summary of the energy and exergy balances were already given in the main report in table 5.3. The energy and exergy stream values for the case of ATR T = 975°C can be seen in table C.4 and table C.5.

The other important information for completing the energy and exergy balances are the electricity generation values. These values can be seen in table C.6.

The efficiencies that were used for the turbines are accounted for by Williams & Larson (1993) and Smith *et al.* (1996). The highest possible conversion for a combined cycle were used with the incineration of the gas in a gas turbine to generate steam. This steam is again used in a steam turbine to generate electricity. This was taken from Williams & Larson (1993).

The steam turbine efficiencies (Smith *et al.*, 1996) were obtained from the best efficiency values of current steam turbines.

The generation of electricity for the other scenario cases can be seen in the main report in figure 5.12.

Table C.4: Energy and exergy stream values for the case of ATR T=975°C

Property (Watt)	15	AIR	DISTFEED	ENVWATER	FRESH	FTFEED	OILWATER
Chemical Enthalpy	5.30E+08	-2.00E+04	3.63E+08	-8.01E+07	7.10E+08	6.81E+08	2.46E+08
Mix Enthalpy	-5.87E-08	-9.41E+01	6.54E+05	0.00E+00	2.55E+05	1.61E+05	1.45E+05
Physical Enthalpy	5.93E+07	2.62E+02	5.60E+07	-4.11E+01	2.02E+08	3.02E+07	4.32E+07
Total Enthalpy	5.90E+08	-1.99E+04	4.20E+08	-8.01E+07	9.13E+08	7.12E+08	2.89E+08
Chemical Exergy	7.94E+08	3.47E+06	6.14E+08	1.64E+06	9.78E+08	8.66E+08	2.98E+08
Mix Exergy	-1.12E+07	-3.15E+06	-1.07E+07	0	-2.04E+07	-1.21E+07	-3.92E+05
Physical Exergy	3.45E+07	-80638.1	3.31E+07	-51.05045	1.15E+08	4.06E+07	1.48E+07
Total Exergy	8.18E+08	2.37E+05	6.36E+08	1.64E+06	1.07E+09	8.95E+08	3.13E+08

Table C.5: Energy and exergy stream values (continued) for the case of ATR T=975°C

Property (Watt)	OXYGEN2	PRODUCTH	PUREGAS	RECYCLE	REF-A	REFFEED	STEAM
Chemical Enthalpy	-5.16E+03	1.69E+08	6.89E+08	9.42E+07	6.08E+08	7.83E+08	-7.60E+07
Mix Enthalpy	1.98E+01	3.24E+04	1.28E+04	2.29E+05	2.82E+05	3.61E+04	0.00E+00
Physical Enthalpy	1.10E+07	2.31E+06	9.20E+06	1.08E+06	2.72E+08	9.23E+07	1.03E+08
Total Enthalpy	1.10E+07	1.71E+08	6.98E+08	9.55E+07	8.81E+08	8.75E+08	2.69E+07
Chemical Exergy	2.05E+06	1.81E+08	7.16E+08	2.58E+08	8.68E+08	9.74E+08	1.55E+06
Mix Exergy	-3.49E+05	-42424.07	-5.67E+05	-5.28E+06	-2.06E+07	-9.33E+06	0
Physical Exergy	9.46E+06	6.59E+05	1.13E+07	1.24E+07	1.72E+08	7.06E+07	3.77E+07
Total Exergy	1.12E+07	1.82E+08	7.26E+08	2.66E+08	1.02E+09	1.04E+09	3.93E+07

Table C.6: Electricity balance for the case of ATR T=975°C

UNIT	Exergy in (Watt)	Exergy out (Watt)	Electr. generated (Watt)	Efficiency	Electr. generated (GJ/t C5-C25 product)
Tail Gas Combustion	5.83E+07	2.91E+07	2.91E+07	0.50	2.8689
Sup. steam turbine	2099300.00	1.47E+06	6.30E+05	0.70	0.0620
Sat. steam turbine	1.17E+07	8.19E+06	3.51E+06	0.70	0.3455

Appendix D

Exergy analysis results

D.1 Internal exergy loss

The exergy results from the Exercom routines were used to calculate the irreversibility of each process unit. The exergy balance for each unit will be shown in this section only for the case of ATR T = 975°C.

The irreversibilities were calculated by using equation 2.19. The duties associated with each unit can be seen in table D.1.

Table D.1: Work duties of important unit processes for ATR T = 975°C

Process Unit	Duties (GJ/ton product)
Blower	0.0987
Water separation cooler	-17.0722
FT-Reactor	-12.0139
Steam generator	1.4572
FT-Reactor preheater	2.7096
ATR feed preheater	8.0383
Total water pumped	0.2226

D.1.1 The reformer irreversibility

The ATR was modelled with no external heat supplied to the reformer. All the heat supplied to the ATR were by means of feed preheating (with exhaust gases) and methane burnt in the ATR. After applying the exergy balance (equation 2.19) to the reformer (with the irreversibility of the mixing of the feed included) an irreversibility of 6.52 GJ/ton

product (where the product is defined as the C_1–C_{25} cut produced in the work-up) was obtained.

D.1.2 The ATR feed preheater irreversibility

The amount of feed preheating to the ATR were done without taking into consideration the effect of sooting. With this assumption, a two stream heat exchanger model was used in Aspen Plus with a design constraint on the outlet temperature of the cold stream at (T_{ref} - 75)°C. This was a rough estimation without any mean-temperature driving force (ΔT) and without any consideration of the transport equation:

$$Q = UA\Delta T_m \tag{D.1}$$

where U is the overall heat transfer coefficient, A is the area for heat transfer and ΔT_m is the mean temperature-driving force for heat transfer.

Equation 2.19 were used on the heat exchanger only considering the two input exergy flows and the two output exergy flows. No internal heat losses were considered. The resulting irreversibility was 0.896 GJ/ton product.

D.1.3 The steam generator irreversibility

Environmental water are pressurised (by a pump) to 24 bar and saturated to vapour (2800.9 kJ/kg, 24 bar) by the heat from the Fischer-Tropsch reactor. This saturated vapour steam is then superheated (h=3297.5 kJ/kg, 24 bar) by the reformer tailgas. The design constraint of 430°C was put on the cold stream outlet temperature. This results in saturated vapour being heated from 222°C to 430°C which is superheated steam at the correct temperature and pressure for feed to the reformer.

The amount of saturated steam that is generated by the FT reactor is 163006 kg/hr. The amount of heat available from the hot reformer outlet gas can superheat 118000 kg/hr of saturated steam. Thus 163006 - 118000 = 45006 kg/hr of saturated steam can be exported to the steam turbines for electricity generation.

But of the 118000 kg/hr of superheated steam generated, only 112010 kg/hr is necessary as feed to the ATR. This then implies a superheated steam export of 5990 kg/hr which is also used for electricity generation.

The irreversibility of the steam generator was calculated with the exergy balance. The balance consisted of the two inlet and two outlet exergy flows to the steam generator.

The irreversibility was 0.217 GJ/ton product.

D.1.4 The Fischer-Tropsch (FT) reactor irreversibility

The thermal exergy was calculated by multiplying the FT reactor duty with the Carnot factor. This can be seen in equation D.2. T_r was taken as 533K and T_0 as 298K.

$$Q \cdot (1 - \frac{T_0}{T_r}) \tag{D.2}$$

After applying the exergy balance (equation 2.19) over the FT reactor an irreversibility of 2.29 GJ/ton product was obtained.

D.1.5 The work-up irreversibility

The irreversibility of the work-up unit was not calculated. since this unit was not yet modelled in detail and since the condenser temperature in the distillation column was close to the reference temperature. The condenser was thus a pseudo unit to model the condenser of the separation column (the Sep block was used in Aspen Plus). Therefore the irreversibility of the condenser was not calculated.

D.1.6 The blower irreversibility

The work exergy was taken as equal to the blower duty. After applying the exergy balance over the blower an irreversibility of 0.025 GJ/ton product was obtained. This loss would have been much greater if the blower was not modelled as isentropic in Aspen Plus. The isentropic compressor efficiency was kept at the default value of 0.72.

D.2 External exergy loss

The external exergy losses are shown in table D.2.

As can be seen from table D.2, the waste streams (or streams not associated with product streams) are included in external exergy losses. The purge combusted stream refers to the purge stream in the recycle loop that is combusted in the combined cycle to produce electricity. An attempt was made to utilise the maximum amount of exergy available from each waste stream in the process.

Table D.2: External exergy losses for ATR T = 975°C case

Stream	Exergy loss (GJ/ton product)
N_2 stream in oxygen separation	1.398
H_2O separated before FT reactor	0.178
Water condensed after used as steam	0.223
Purge combusted stream (for electricity)	5.565